frontiers in Earth Science

ORIGINAL RESEARCH
published: 11 November 2021
doi: 10.3389/feart.2021.772374

Mesoscopic and Microscopic Magmatic Structures in the Quxu Batholith of the Gangdese Belt, Southern Tibet: Implications for Multiple Hybridization Processes

Xuxuan Ma[1,2], Zhongbao Zhao[1,2], Wenrong Cao[3], He Huang[1], Fahui Xiong[1,2], Tarryn Cawood[4] and Haibing Li[1,2]*

[1]Key Laboratory of Deep-Earth Dynamics of Ministry of Natural Resources, Institute of Geology, Chinese Academy of Geological Sciences, Beijing, China, [2]Southern Marine Science and Engineering Guangdong Laboratory, Guangzhou, China, [3]Department of Geological Sciences and Engineering, University of Nevada, Reno, NV, United States, [4]Department of Earth Sciences, University of Southern California, Los Angeles, CA, United States

OPEN ACCESS

Edited by:
Yibo Yang,
Institute of Tibetan Plateau Research (CAS), China

Reviewed by:
Yuanku Meng,
Shandong University of Science and Technology, China
Liang Guo,
China University of Geosciences Wuhan, China
Chao Zhang,
Northwest University, China

***Correspondence:**
Xuxuan Ma
xuxuan.ma@hotmail.com

Specialty section:
This article was submitted to Structural Geology and Tectonics, a section of the journal Frontiers in Earth Science

Received: *08 September 2021*
Accepted: *19 October 2021*
Published: *11 November 2021*

Citation:
Ma X, Zhao Z, Cao W, Huang H, Xiong F, Cawood T and Li H (2021) Mesoscopic and Microscopic Magmatic Structures in the Quxu Batholith of the Gangdese Belt, Southern Tibet: Implications for Multiple Hybridization Processes. Front. Earth Sci. 9:772374. doi: 10.3389/feart.2021.772374

The Quxu batholith of the Gangdese magmatic belt, southern Tibet, comprises predominantly Early Eocene calc-alkaline granitoids that feature a variety of types of magmatic microgranular enclaves and dikes. Previous studies have demonstrated that magma mixing played a crucial role in the formation of the Quxu batholith. However, the specific processes responsible for this mixing/hybridization have not been identified. The magmatic microgranular enclaves and dikes preserve a record of this magma mixing, and are therefore an excellent source of information about the processes involved. In this study, mesoscopic and microscopic magmatic structures have been investigated, in combination with analyses of mineral textures and chemical compositions. Texturally, most of the enclaves are microporphyritic, with large crystals such as clinopyroxene, hornblende, and plagioclase in a groundmass of hornblende, plagioclase, and biotite. Two types of enclave swarms can be distinguished: polygenic and monogenic swarms. Composite dikes are observed, and represent an intermediate stage between undisturbed mafic dike and dike-like monogenic enclave swarms. Our results reveal three distinct stages of magma mixing in the Quxu batholith, occurring at depth, during ascent and emplacement, and after emplacement, respectively. At depth, thorough and/or partial mixing occurred between mantle-derived mafic and crust-derived felsic magmas to produce hybrid magma. The mafic magma was generated from the primitive mantle, whereas the felsic end-member was produced by partial melting of the preexisting juvenile crust. Many types of enclaves and host granitoids are thus cogenetic, because all are hybrid products produced by the mixing of the two contrasting magmas in different proportions. In the second stage, segregation and differentiation of the hybrid magma led to the formation of the host granitoids as well as various types of magmatic microgranular enclaves. At this stage, mingling and/or local mixing happened during ascent and emplacement. In the final stage, mafic or hybrid magma was injected into early fractures in the crystallizing and cooling pluton to form dikes. Some dikes remained undisturbed, whereas others experienced local

mingling and mixing to form composite dikes and eventually disturbed dike-like monogenic enclave swarms. In summary, our study demonstrates the coupling between magmatic texture and composition in an open-system batholith and highlights the potential of magmatic structures for understanding the magma mixing process.

Keywords: magmatic structure, magmatic microgranular enclave, multiple hybridizations, magma mixing, Quxu batholith, Gangdese, synplutonic dike

INTRODUCTION

Magma mixing is an important process in the genesis of calc-alkaline granitoids worldwide (Castro et al., 1990; Janoušek et al., 2000; Farner et al., 2017). The occurrence of such mixing between mafic and felsic magmas can be demonstrated using igneous geochemistry. In particular, whole-rock and mineral radiogenic isotopes have proved to be an invaluable proxy for distinguishing the end-members of magma mixing, based on the assumption that mantle-derived mafic magmas are isotopically juvenile and crust-derived felsic melts are more evolved (Barbarin, 2005; Liu et al., 2013; Gao et al., 2016). In addition, magma mixing may result in intrusive suites ranging from mafic through intermediate to felsic that show a trend of increasing $\varepsilon_{Nd}(t)$ and $\varepsilon_{Hf}(t)$ values and decreasing $(^{87}Sr/^{86}Sr)_i$ ratios with increasing bulk rock SiO_2 contents (Jiang et al., 2018). However, a purely geochemical approach has limitations. For example, isotopes alone cannot be used to distinguish the original end members if the felsic melts are derived from very juvenile crust, such as those in the Gangdese belt, southern Tibet (Mo et al., 2005; Ji et al., 2009; Ma et al., 2017a; Wang et al., 2019b). In such a case, an integrated study of field relations (mesoscopic and microscopic magmatic structures), petrography, and mineralogical observations is required to provide convincing support for magma mixing in the genesis of calc-alkaline granitoids. The mesoscale evidence of mixing between mafic and felsic magmas could include preserved synplutonic dikes, magmatic microgranular enclaves (MMEs), MME swarms, and gradational compositional variation of plutons from gabbro to granite (Foster and Hyndman, 1990; Jayananda et al., 2009; Jayananda et al., 2014).

Magmatic microgranular enclaves are common in calc-alkaline granitoids formed in the subduction-related circum-Pacific arc and are abundant in most of the Cordilleran granitoid plutons (Wiebe et al., 2002; Barnes et al., 2021). These MMEs provide evidence for the role of mafic magmas in the initiation and formation of calc-alkaline granitoid magmas in a continental arc and thus their origin is important in interpreting the history of batholiths around the globe. Although significant progress has been made, the origin of MMEs remains controversial. One model suggests that MMEs are early crystallized cumulates of the same magma system (autolith or cogenetic xenoliths) (Dodge and Kistler, 1990; Niu et al., 2013; Zhang and Zhao, 2017; Xu et al., 2021), whereas others propose that they are a by-product of magma mixing of mantle-derived and crustal melts (hybrids) (Barbarin and Didier, 1992; Barbarin, 2005; Barnes et al., 2021). Generally, most of the MMEs hosted within the granitoids, are intermediate in composition (dioritic to tonalitic, with some granodioritic), and are therefore thought to have been produced by the latter process (Jin, 1986; Barbarin, 2005). In addition, whether MMEs with intermediate composition could continue to mix with the host granitoid magma during their ascent remains unclear. In such a case, an integrated study of mineral chemistry and disequilibrium textures (microstructure) is required to shed light on potential further magma mixing between the dioritic-granodioritic enclaves and their host granitoid magma before their arrival at the emplacement depth (Vernon, 1990; Hibbard, 1991; Tobisch et al., 1997; Ma et al., 2017a).

Previous workers have demonstrated that magma mixing did occur during the formation of the Quxu batholith, through observations of geochronological, geochemical, isotopic, and field data, along with mineralogical structures and textures (Mo et al., 2005; Dong et al., 2006; Ma et al., 2017a; Shu et al., 2018; Wang et al., 2019b; Ma et al., 2020a; Wen et al., 2021). However, the specific processes that resulted in this magma hybridization/mixing remain unclear. In particular, it is unknown how many distinct stages of magma hybridization may have occurred.

In this study, we investigate the mesoscopic and microscopic structures and mineral compositions of MMEs to reveal the different stages of magma mixing in the Quxu batholith of the central Gangdese belt, southern Tibet. Our study shows that different types of MME, from dike-like enclave swarms to ellipsoidal enclaves, manifest magma mixing at different crustal levels. This indicates that magma mixing occurred in several stages over a period of time, both before and during emplacement of the MMEs and their host magma.

GEOLOGICAL SETTING

The Tibetan Plateau, sandwiched by the northern Tarim and North China cratons and the southern Indian continent, formed through the sequential accretion of terranes to the southern margin of the Eurasian continent (Xu et al., 2015; Yin and Harrison, 2000). These terranes, from north to south, include the Kunlun, Songpan-Ganze, Qiangtang, Lhasa, and Tethyan Himalayan terranes, which are separated by the Anymaqen-Kunlun, Jinsha, Bangong-Nujiang, and Indus-Yarlung Tsangpo suture zones, respectively (**Figure 1**; Kapp and DeCelles, 2019).

The Lhasa terrane (**Figure 1**), located in southern Tibet, is separated from the northern Qiangtang terrane and the southern Tethyan Himalayan terrane by the Bangong-Nujinag and Indus-Yarlung Tsangpo suture zones, respectively. It extends ca. 2,000 km E-W along strike, with a width of 300–100 km. The Lhasa terrane, as an integral part of the Cimmerian continent, is

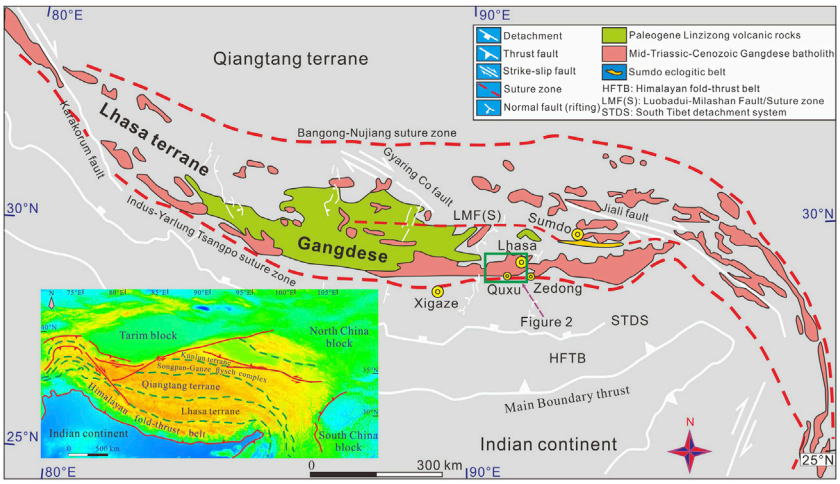

FIGURE 1 | Simplified geological map of the Gangdese magmatic belt in the southern Lhasa terrane showing the location of the Quxu batholith.

speculated to have rifted off from the Gondwana landmass in the Early Permian during dispersal of the Pangea supercontinent (Veevers and Tewari, 1995; Ueno, 2003; Meng et al., 2016; Meng et al., 2018b; Ma et al., 2020b). It then drifted northward as the Tethyan Ocean was closed, before its final collision with the Asian continent along the Bangong-Nujiang suture zone in the Cretaceous. Recent studies reveal that the Lhasa terrane is a composite block with differences between the northern, central, and southern sub-terranes (Yang et al., 2007; Zhu et al., 2013). The northern and southern Lhasa terranes are distinguished by a lack of pre-Mesozoic basement. In contrast, the central Lhasa terrane is characterized by the presence of the Precambrian basement, namely the Nyainqêntanglha Group amphibolite-facies metamorphic sequences (Allègre et al., 1984; Zhu et al., 2011).

The southern Lhasa sub-terrane, which is separated from the central Lhasa basement by the Luobadui-Milashan fault, predominantly comprises Mesozoic and Cenozoic igneous rocks (Zhu et al., 2011; Ma et al., 2021a). This magmatic belt is known as the Gangdese magmatic belt or the Gangdese batholith, comprised of subduction and collision-related plutons and equivalent volcanic rocks now exhumed as a tilted magmatic orogen (Cao et al., 2020). Existing geochronological data identify four distinct episodes of magmatism in the Gangdese belt at 240–150, 100–80, 65–40, and 30–13 Ma (Ji et al., 2009; Ma et al., 2018; Zhu et al., 2019; Ma et al., 2020b; Meng et al., 2020). The 240–150 and 100–80 Ma magmatism is ascribed to be associated with the subduction of the Neotethyan oceanic lithosphere (Wen et al., 2008; Ji et al., 2009; Xie and Tang, 2021). The 65–40 Ma magmatism was probably formed during the tectonic transition from ocean-continent subduction to continent-continent collision (Mo et al., 2003; Ma et al., 2017a; Tang et al., 2021). The Miocene (33–13 Ma) magmatism is represented by scattered collision-related adakites, which resulted from partial melting of a thickened mafic crust due to the Indo-Asian collision (Chung et al., 2005; Ji et al., 2009).

As an important part of the Gangdese belt, the Quxu batholith has received much attention among the geological community (**Figure 2**; Harrison et al., 1992; Ji et al., 2009; Cao et al., 2020; Ma et al., 2017a). It primarily consists of Eocene granitoids, diorite, tonalite, quartz diorite, gabbro, and gabbronorite. Previous geochronological results reveal that the plutons of the Quxu batholith crystallized predominantly during the Early Eocene, ranging from 55 to 45 Ma, and peaking at ca. 50 Ma (**Figure 2**). As the main body of the Quxu batholith, the dioritic-tonalitic-granodioritic-monzogranitic suite is marked by the widespread occurrence of MMEs (**Figure 3**). Locally, MMEs account for 80% or more of the outcrop, but decrease to ~20% in most of the remaining areas (**Figure 3**). Previous studies reveal that the MMEs crystallized coevally with their host granitoids, largely at ca. 50 Ma (Mo et al., 2005; Ma et al., 2017a; Wang et al., 2019b). Several lines of evidence indicate that the MMEs and their host granitoids formed from hybrid magma: a linear variation trend among gabbros, MMEs, and granitoids is shown in Harker diagrams (Dong et al., 2006), as well as in a series of hyperbolic mixing arrays (Ma et al., 2017a). In addition, similar REE patterns, trace element spider distributions, and zircon epsilon Hf values for gabbros, MMEs, and granitoids provide more evidence for magma mixing (Dong et al., 2006; Wang et al., 2019b).

FIELD OBSERVATIONS OF MESOSCOPIC MAGMATIC STRUCTURES

Synplutonic Dikes and/or Monogenic Enclave Swarms

Numerous synplutonic dikes (generally, mafic in composition) are found in the Quxu batholith, with thicknesses ranging from several centimeters to meters. These dikes vary from coherent, homogeneous dikes with regular wallrock contacts, through composite dikes, to swarms of magmatic enclaves with an overall dike-like shape. The composite dikes are especially

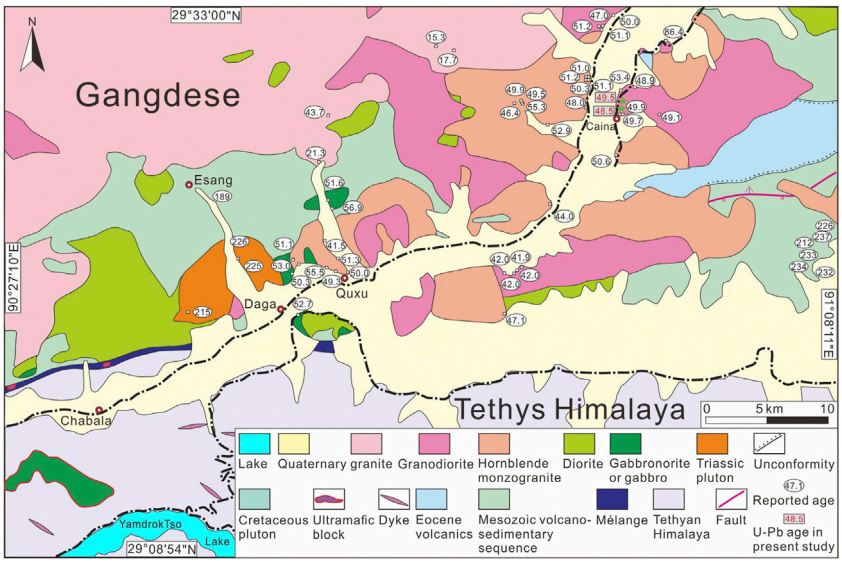

FIGURE 2 | Geological map of the main body of the Quxu batholith in the Gangdese belt. The reported zircon U-Pb data are compiled from Huang et al. (2021), Ji et al. (2009), Ma et al. (2017a, 2017b), Meng et al. (2018b), Mo et al. (2005), Wang et al. (2016), Wang et al. (2019a, 2019b), Wen et al. (2008). These dating results demonstrated that the Quxu batholith was mainly formed between 55 and 45 Ma.

abundant, displaying fine-to coarse-grained, equigranular to porphyritic textures and are characterized by back-veining, necking, and gradational variations in composition (**Figure 3**). In some cases, the dikes are boudinaged or fragmented into numerous small magmatic enclaves. These small enclaves are ellipsoidal in shape but oriented along the dike striking direction (**Figures 3A–D**). Synplutonic dikes are typically interpreted as injections into crystallizing felsic magma chambers and are common in Phanerozoic circum-Pacific calc-alkaline batholiths in arc settings (Foster and Hyndman, 1990; Ghani, 1998; Barbarin, 2005). We therefore interpret the synplutonic dikes in the Quxu batholith as the result of mafic or intermediate magma injected into a partially crystallized felsic host.

Contacts Between Different Plutonic Units

In the Quxu batholith, a variety of contact relationships are observed between the coeval plutons or units (**Figure 4**). Contacts between the gabbroic and granitoid rocks are sharp (**Figure 4C**), but contacts between the MMEs and their granitoid host rocks are gradational (**Figures 4D–F**). Sharp contacts develop when the host rock has already cooled and solidified before emplacement of the second batch of magma, and thus indicate that different pulses of magma played a role in the formation of the Quxu batholith. In contrast, gradational contacts form when both batches of magma are still fully or partially liquid, allowing local mixing. Gradational contacts in the Quxu batholith thus indicate magma mixing and hybridization, at different crustal levels. Furthermore, gradational contacts are also observed in the synplutonic dikes (**Figure 3F**), which are more mafic in the center and less mafic near the margins. This phenomenon reveals that the host magma was not completely crystallized when the mafic magma was injected. Heat from the suprasolidus host granitoids likely slowed the cooling and crystallization of the mafic magma and thus promoted crystal fractionation within the injected magma dikes.

Magmatic Flow

Magmatic flow is required for magma mixing to occur between MMEs and their enclosing granitoids (Vernon, 1990). Although magmatic flow ceased when the magmas cooled and became fully crystallized, evidence for it is preserved in the form of magmatic flow structures. In the Quxu batholith, magmatic flow structures are represented by the orientation of lenticular enclaves (**Supplementary Figure S1A**), the orientation of minerals in host granitoids (e.g., hornblende) (**Supplementary Figures S1B–D, J**), the elongation of enclaves along the magmatic foliation (**Supplementary Figure S1H**), the flow tails surrounding the enclaves (**Supplementary Figures S1E–G, I**), and the orientation of hornblendes in the enclaves (**Supplementary Figures S1K–L**). These magmatic flow structures suggest that the MMEs and their host granitoids co-existed in the plastic state and flowed together along the flow track of the host magma (Jayananda et al., 2014; Ma et al., 2017a). The flow structures are not a by-product of solid-state deformation, because the host plutons show no evidence of solid-state deformation.

Magmatic Faults and Folds

Faults and folds are typically formed by solid-state deformation, which may occur under brittle or ductile conditions, and may be local or regional in scale. However, apparent faults and folds can also be found in the undeformed plutons around the globe (Paterson et al., 2018). These faults and folds are thus actually magmatic flow structures, formed during suprasolidus magma

FIGURE 3 | Field photos showing the various types of enclave swarms and dikes. **(A)** A dike-like monogenic swarm consists of similar MMEs enclosed in granodiorite. These MMEs have similar shapes and compositions and are oriented in the same direction. **(B)** A polygenic swarm consists of many types of MMEs with different sizes and shapes. Only a weak preferred orientation could be seen. **(C)** A monogenic swarm consists of similar enclaves, but no obvious orientation. **(D)** A monogenic swarm consists of similar enclaves with obvious orientation along the flow direction of host magma. **(E)** Synplutonic dike, occasionally, with lobate contacts and flow tails. **(F)** Close-up of **(E)** showing the compositional gradation from the core to the margin of the synplutonic dike. **(G)** Close-up of **(E)** showing the embayed host within the synplutonic dike. **(H)** Synplutonic dike showing the lobate contacts. The width of the dike varies along its strike due to necking and embaying structure.

flow within a pluton, without any additional imposed solid-state deformation.

As shown in **Figure 5**, a variety of magmatic faults and folds occur in the fresh and undeformed granitoid plutons in the Quxu batholith. These structures include magmatic strike-slip shear zones (**Figure 5A**), magmatic normal fold (**Figure 5B**), magmatic fold (**Figure 5C**), sigma-shaped MMEs indicative of slide (**Figures 5D,E**) or thrust (**Figure 5F**) shear, strongly folded magmatic enclave (**Figure 5G**), and elongate enclaves (**Figures 5H–J**). All of these structures are magmatic in origin, without evidence for intra-crystal plastic deformation (such as deformation lamellae, deformation twin, banded extinction, undulatory extinction, subgrain formation, etc.). In addition, all these structures are local, without long-distance extensions. They therefore formed during local magma flow within the pluton, possibly due to local magmatic flow during emplacement or gravity imbalances such as magmatic collapse (Alasino et al., 2019; Ardill et al., 2020).

Double and/or Multiple Enclaves

Double and multiple enclaves, comprising multiple domains of different composition and/or texture, are typical indicators of

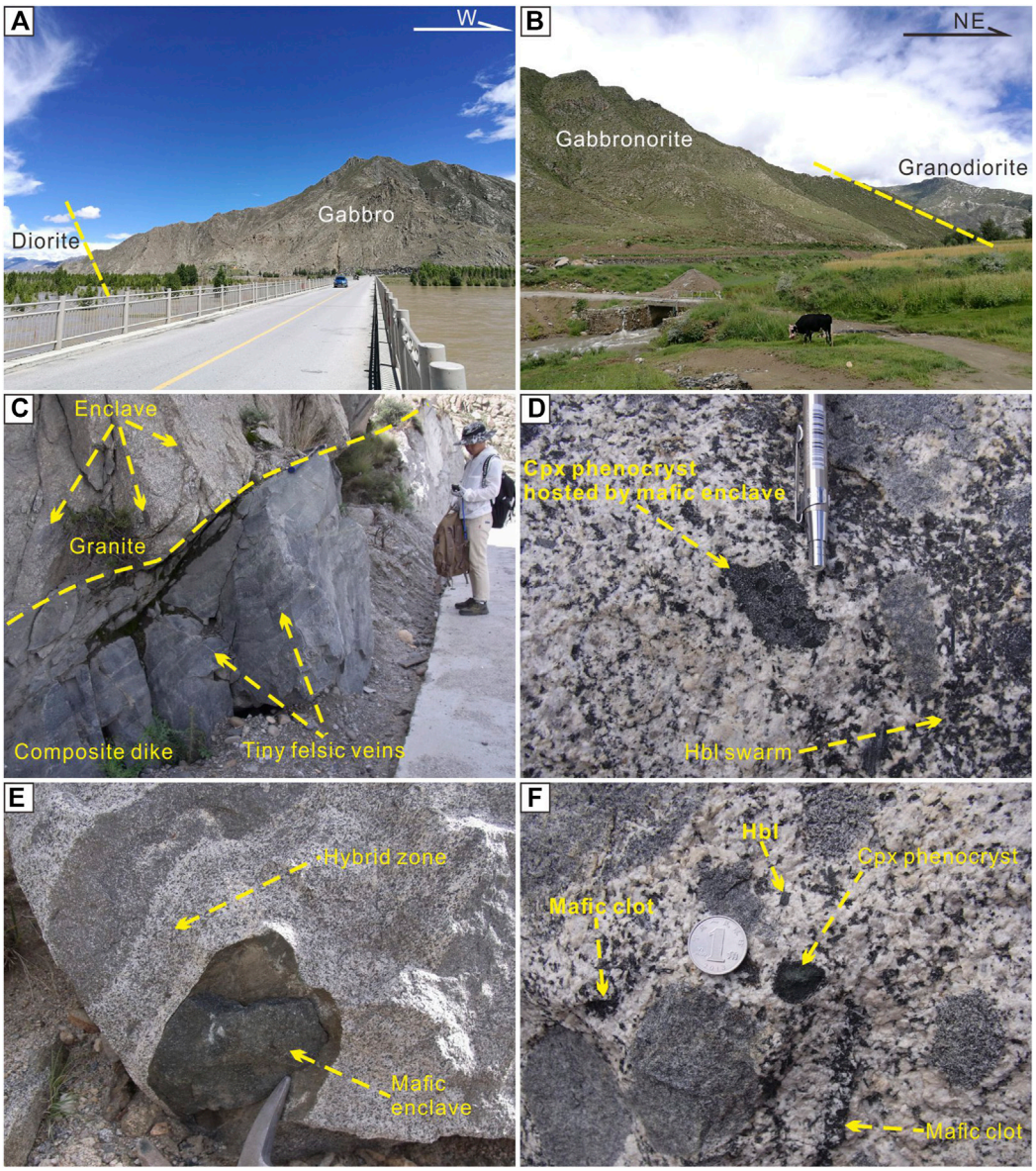

FIGURE 4 | Field photos showing the contact between different rock types. **(A)** The contact between the gabbro and the diorite in the south of the Quxu bridge. **(B)** The contact between gabbronorite and granodiorite in the town of Daga. **(C)** A mafic dike intruded into the crystallized monzogranite and cut by small scale felsic veins, formed during the latest stage of hybridization. **(D)** A polygenic swarm of enclaves, mafic to intermediate in composition. **(E)** The mixing zone between a mafic enclave and an intermediate enclave. **(F)** Polygenic swarm including intermediate enclave, mafic clots, and large clinopyroxene crystal.

magma mixing (Castro et al., 1990; Pin et al., 1990; Vernon, 2007; Liu et al., 2013; Ma et al., 2017a). Double enclaves are commonly present in the granitoid plutons of the Quxu batholith (**Figure 6**). Some double enclaves have dark, megacryst-poor centers surrounded by lighter zones relatively rich in plagioclase megacrysts (**Figures 6A, C, D, F**). These cores may represent retained blobs of the non-hybrid mafic magma, whereas the outer zones resulted from the mixing of varied proportions of felsic and mafic magmas. In contrast, some double enclaves have light, megacryst-rich cores surrounded by dark zones (**Figure 6B**). Correspondingly, the cores may represent hybrid magma resulted from the mixing of felsic and mafic components. All these double and multiple enclaves preserve their original outline, revealing an incomplete hybridization between the felsic and mafic magmas. Interestingly, some double enclaves have a rim zone enriched in covellite (**Figure 6G**), which could be a by-product of mixing between the mafic and felsic magmas.

Composite/Fragmented Dikes

Various mechanical processes may concentrate MMEs to form pipes or dikes. These dikes consisting of MME of various types and sizes enclosed in a mafic aggregate are described as composite

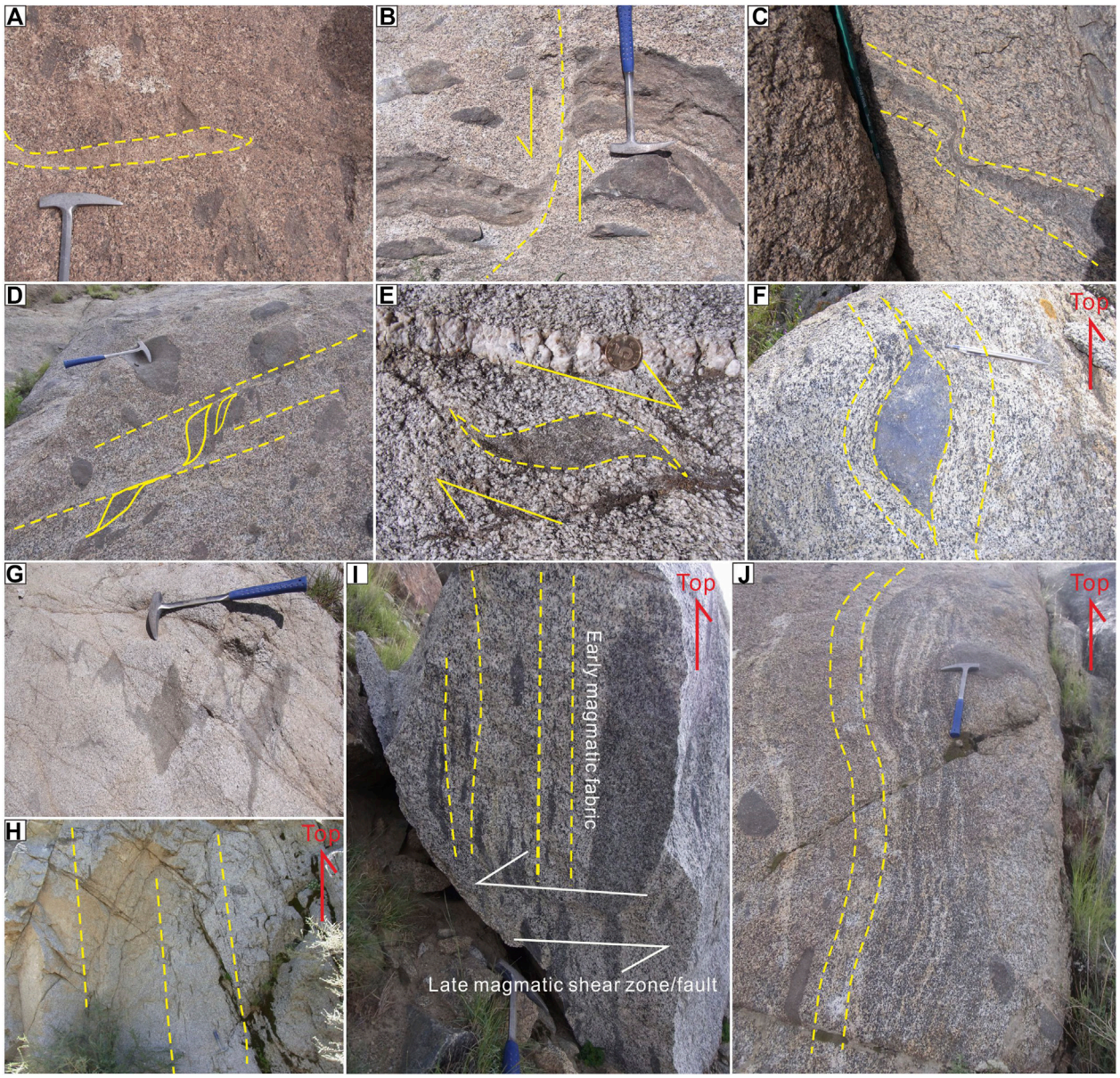

FIGURE 5 | Field photos showing the magmatic faults, folds, and schlieren structures. **(A,B)** Magmatic fault represented by a leucocratic zone. **(C)** Magmatic fold. **(D–F)** Magmatic faults, resembling ductile shear zones, with typical σ-type enclaves. **(G)** Magmatic folds, which have folded the enclave into a wave-like form. **(H,I)** Elongated enclaves oriented along the magmatic foliations. These foliations are cut by a second magmatic fabric. **(J)** An enclave that has been disrupted into schlieren-like ribbons by magmatic flow.

dikes (Reid and Hamilton, 1987). As shown in **Supplementary Figures S2A,B**, the nearly continuous mafic dikes and mafic rocks are divided into angular blocks by the injection of felsic veins with widths ranging from centimeters to decimeters. The contacts of these dikes with enclosing hosts are distinct but neither straight nor sharp. Generally, these contacts are lobate in shape and are diffusive (**Supplementary Figure S2A**). Within individual composite dikes, mafic fragments have similar compositions, whereas the nature of the fragments may vary dramatically from one dike to another.

Net/Back-Veining of Mafic Rocks

Historically, net- or back-veining was thought to represent a salic rheomorphic melt produced by an emplaced sheet of magma in the adjacent host rock (Douglas, 1964). More recently, however, net/back-veining has been shown to result from magma hybridization between mafic and felsic melts (Barbarin and Didier, 1992). In general, the mafic magma has a higher temperature than the host granitoid magma. The injection of mafic magma with higher temperature thus heats the crystallizing, cooling granitoid magma to form a felsic melt.

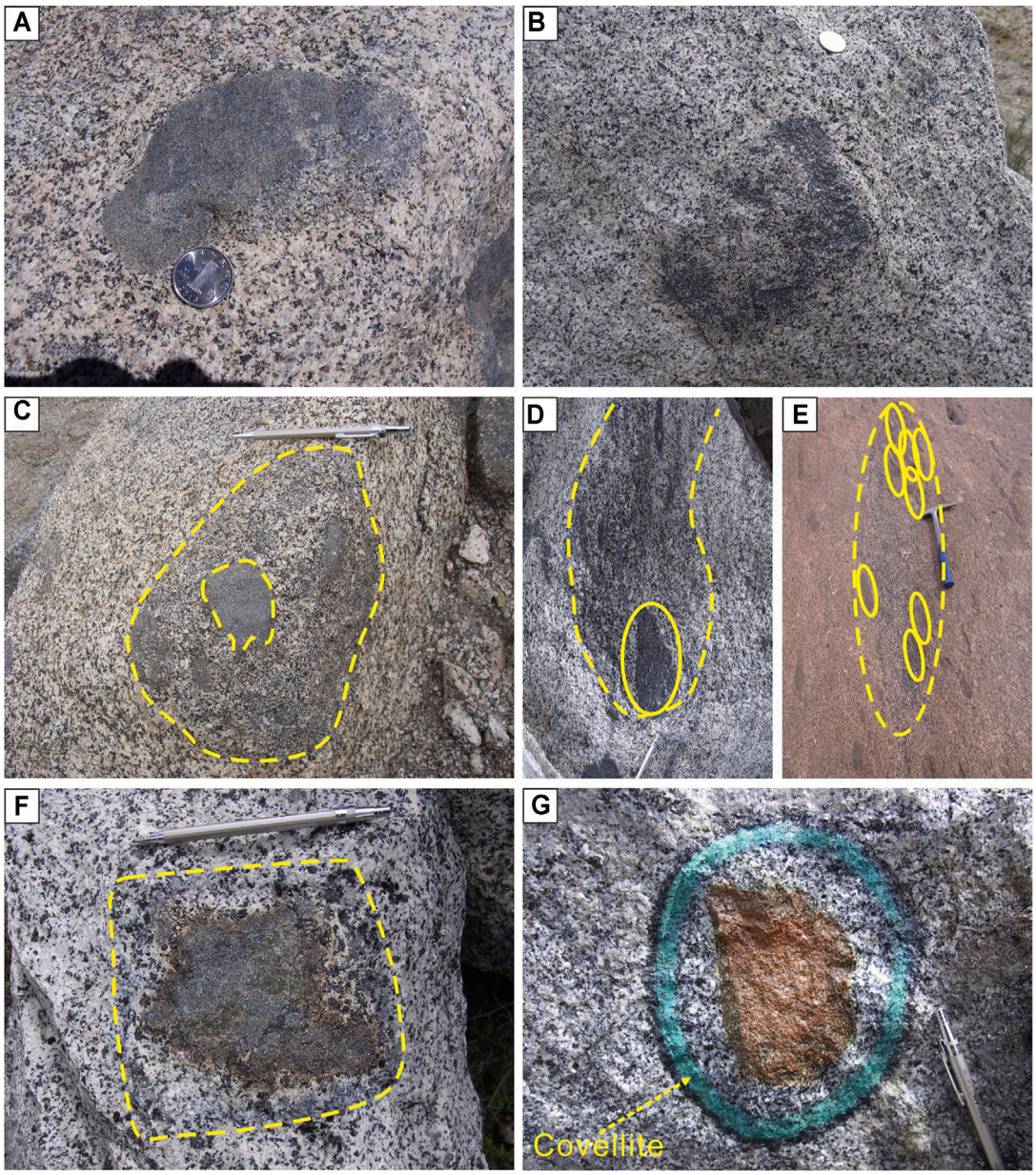

FIGURE 6 | Field photos showing the composite enclaves. **(A,B)** Variable interaction of the enclaves with the enclosing host rock, with the lower right side of the enclave exhibiting a greater degree of interaction with the host. **(C–F)** Double enclaves with the outline of the original enclaves. **(G)** An enclave showing a rounded margin of copper, revealing the interaction of the enclave with the host granitoid magma.

This newly formed felsic melt then intrudes the pinched regions of the crystallizing mafic magma (Sylvester, 1998; Jayananda et al., 2009). Several examples of net/back-veining are observed in the Quxu batholith. **Supplementary Figure S2C** illustrates ribbon-like schlieren of mafic material with smooth margins, interpreted as having formed when the mafic magma was stretched and disaggregated while still in a plastic state. In **Supplementary Figures S2D,E**, the mafic magma intruded the felsic magma and form numerous small mafic blobs within it. Along the mafic/felsic contacts, net-veining cut the cooling mafic magma and formed small-scale leucosome veins. In summary, these occurrences of net-veining in the Quxu batholith are interpreted to have been produced by late injections of large volumes of mafic magma into partially crystallized granite and the interaction between the two magmas at the emplacement level (Barbarin and Didier, 1992).

Mineral Capture

As mentioned above, magmatic flow and a plastic state of the mafic and felsic magmas are prerequisites for magma mixing. Such mixing will also trigger the transfer of minerals from the felsic magma into MMEs (Słaby et al., 2008). In the Quxu

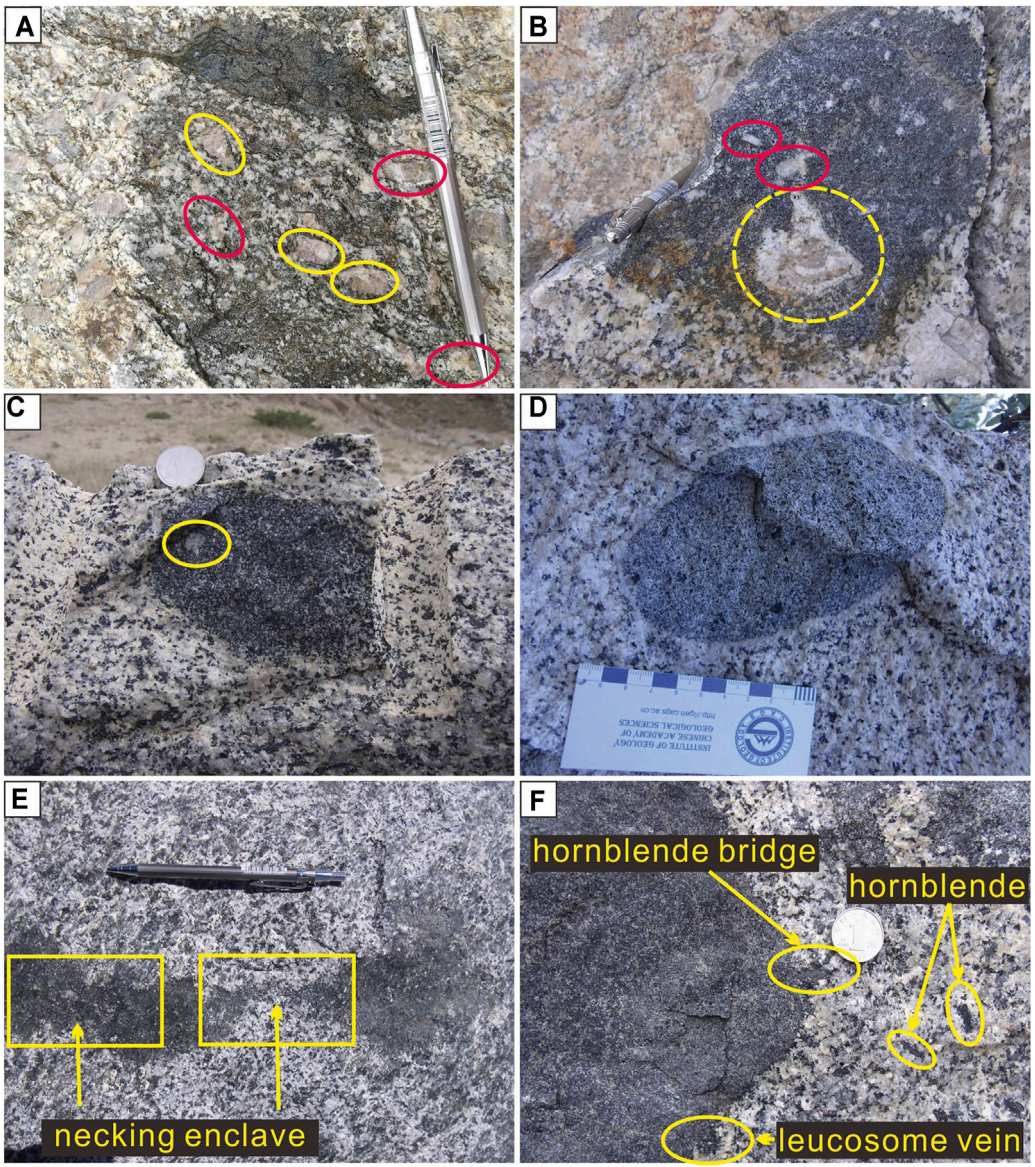

FIGURE 7 | Field photos showing the transfer and bridging of minerals from host magma into enclaves. **(A,B)** Large K-feldspar crystals within the enclaves were captured from the host monzogranite magma. **(C)** Plagioclase phenocrysts within the enclaves were captured from the host dioritic to granodioritic magma. **(D)** An enclave is mantled by a fine-grained leucocratic margin that is characterized by a trachytic texture. This leucocratic margin will prohibit further chemical and mineral exchange. **(E)** An enclave subjected to necking, indicating that the enclave deformed plastically within the host granitoid magma. **(F)** Large hornblende crystal is connecting the enclave and the host, referred to as "hornblende bridge," indicating that both the enclave and the host rock were in the plastic state during hornblende growth. Minor leucosome vein is found between the contrasting components. The leucosome will inhibit further interaction between the enclave and the host granitoids. Euhedral hornblendes are scattered in the host granitoids.

batholith, K-feldspar, plagioclase, and quartz phenocrysts are enclosed within the MMEs (**Figures 7A–C**). These phenocrysts are inconsistent with the typical composition and texture of the mafic to dioritic enclaves, which are otherwise equigranular in texture, comprising microgranular hornblende, plagioclase, and biotite with minor quartz. The phenocrysts are therefore interpreted as having crystallized in the felsic magma and been transferred into the liquid mafic or dioritic enclaves during magma flow and mixing. The plastic state of the enclaves at the time of mixing is marked by the occurrence of necking structures (**Figure 7E**). In addition, the large euhedral hornblende grain in **Figure 7F** likely originated from the host granitoid magma that surrounds the magmatic enclave. However, it is not obviously cross-cut by the MME. It thus resembles a "hornblende bridge" connecting the host granitoids and the MME, indicating their co-existence in a plastic state. The embayments of the MMEs that frequently penetrate the megacryst-rich granitoid magma and trigger the formation of

leucosome margins around the enclave likely also reflect magma mixing under plastic conditions (**Figure 7F**).

ANALYTICAL METHODS

Zircon LA-ICPMS U-Pb Dating

Two samples (xm56-monzogranite and xm63-granodiorite) were collected for zircon LA-ICPMS U-Pb dating. The dated plutons are located in the core of the Quxu batholith and are characterized by the occurrence of many types of MMEs. Thus, their ages are crucial to address the timing of magma mixing in the Quxu batholith. Zircon U–Pb geochronological dating was performed on an Agilent 7500a ICPMS with a NewWave 213 nm laser ablation system at the State Key Laboratory of Mineral Deposits Research, Nanjing University, Nanjing, China. A laser beam of ca. 32 μm and a repetition rate of 5 Hz with a 70% energy condition were employed. Isotopic mass fractionation was corrected using an external standard GEMOC GJ-1 with $^{207}Pb/^{206}Pb$ age = 608.5 ± 1.5 Ma (Jackson et al., 2004). Zircon dating was carried out in runs of fifteen analyses, including approximately 10 sample spots and five zircon standards. The analytical age results were calculated from the raw signal data using the online software GLITTER (ver. 4.4) (www.mq.edu.au/GEMOC). Common lead (Pb) correction was performed through the EXCEL program (ComPbCorr#3-15G) (Andersen, 2002). The U-Pb age calculations and Concordia age plotting were performed through the ISOPLOT/Ex program (ver. 2.49) (Ludwig, 2003). Zircon Th and U concentrations were calculated according to the comparison of relative signal intensity between the standard zircon GJ-1 (Th = 8 ppm and U = 330 ppm) and the zircon samples using the EXCEL program Data Templatev2b from GEMOC. The zircon U-Pb analytical results are listed in **Supplementary Table S1**.

Electron Microprobe Analysis

Representative magmatic plagioclase, amphibole, and clinopyroxene from thin sections of MME samples were selected for electron microprobe analyses (EMPA). Chemical compositions were analyzed using a JEOL JXA-8900 electron microprobe (EMP) with a 5 μm or less probe beam spot diameter, 20 nA beam current, and counting time of 10 s for peak and background under a 15.0 kV accelerating voltage at the Institute of Geology, Chinese Academy of Geological Sciences, Beijing 100037, China. Natural standards were employed for the calculations of the EMPA results. The EMPA analytical results of plagioclase, amphibole, and clinopyroxene are presented in **Supplementary Tables S2–S4**, respectively.

ANALYTICAL RESULTS

Geochronology

Zircon grains from the monzogranite and granodiorite samples are colorless, subhedral-euhedral, and prismatic in shape. The length of zircon grains ranges from 50 to 100 μm with aspect ratios of 1:1–2:1. Most of these zircon grains show clear oscillatory zoning, whereas some have banded zoning. In addition, these zircon grains yield very high Th/U ratios, ranging from 0.79 to 2.09 for the monzogranite and 0.90 to 1.39 for the granodiorite, respectively (**Figure 8**). These observations indicate that the zircon grains are magmatic in origin. Therefore, we interpret their LA-ICPMS U-Pb weighted mean ages as the crystallization ages of the plutons. Twenty-four zircon grains from the monzogranite yield an intercept age of 48.5 ± 0.6 Ma (weighted mean square deviate (MSWD) = 0.52), with a corresponding weighted mean age of 48.2 ± 0.4 Ma (MSWD = 1.6) (**Supplementary Figure S3**). Similarly, 24 zircon grains from the granodiorite yield an intercept age of 49.5 ± 1.2 Ma (MSWD = 0.17), corresponding to a weighted mean age of 48.9 ± 0.4 Ma (MSWD = 0.81) (**Supplementary Figure S3**).

Mineral Textures and Chemical Compositions

Two plagioclase phenocrysts from MMEs were selected for investigation with backscattered-electron imaging (BSE) and EMPA imaging (**Figure 9**). These images reveal that the plagioclase phenocrysts are strongly compositionally zoned, displaying core, mantle, and rim zones with sharply distinct anorthite (An) numbers (core: 35–48, mantle: 78–84, and rim: 36–45). In addition, some plagioclase phenocrysts exhibit resorption textures such as dendritic, poikilitic, sieved-like, and spike-like textures (detailed discussion in the following section).

Several hornblende phenocrysts from MMEs were subjected to BSE imaging, as well as spot and line EMPA analyses (**Figure 10**). Microphotographs and BSE images reveal that relict clinopyroxene form the core of the hornblende phenocrysts. Furthermore, flake-like amphibole and needle-like amphibole are enclosed within the relict clinopyroxene. The EMPA results of the amphiboles fall into the edenite and magnesiohornblende fields in the classification diagram, whereas the amphibole inclusions of the clinopyroxene core belong to silicic edenite or actinolite (**Figure 11**).

DISCUSSION

Mineral Textural and Compositional Disequilibrium of Magmatic Microgranular Enclaves During Magma Mixing

Numerous disequilibrium textures exist in both the MMEs and the host granitoids. In the MMEs, some plagioclase phenocrysts display a strong core-mantle-rim compositional zonation, characterized by sharply distinct An numbers (**Figure 9**). The distinct changes in An number suggest that crystal growth was discontinuous, and that the different zones grew from magmas with different compositions. In addition, some plagioclase phenocrysts exhibit resorption textures such as dendritic, poikilitic, sieved-like, and spike-like textures (**Figures 12A–C**), revealing mafic magma recharge and replenishment (Nelson and Montana, 1992; Mitchell et al., 1998). The mixing or interactions

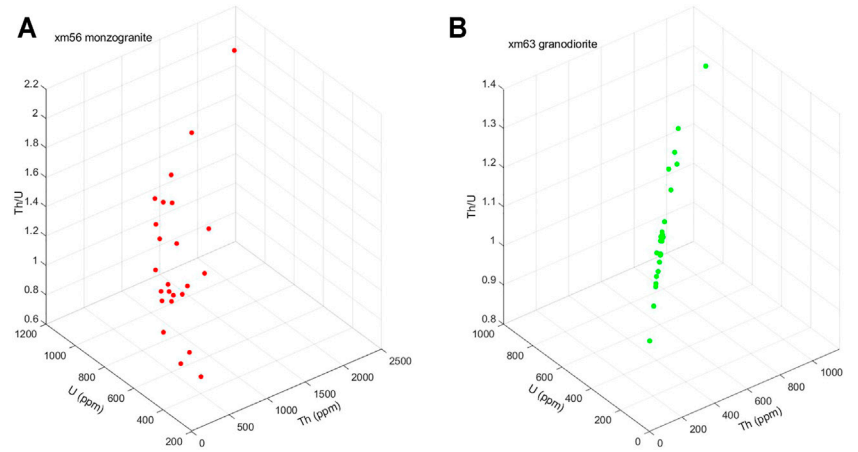

FIGURE 8 | Diagrams of zircon Th, U, and Th/U ratios. **(A)** Zircon grains from sample xm56 monzogranite in the Caina intrusive complex of the Quxu batholith. **(B)** Zircon grains from sample xm63 granodiorite in the Caina intrusive complex, Quxu batholith.

between different magma batches is the best condition for the abovementioned textures (Browne et al., 2006).

The core-rim texture of clinopyroxene-amphibole is another clue for disequilibrium indicative of magma mixing for the MMEs (**Figures 12D–F**). There is no obvious transitional or gradational zone between the clinopyroxene core and the hornblende mantle, except for some amphibole patches or inclusions within the clinopyroxene relict core (**Figure 10**). These observations suggest that the hornblende mantle is not an alteration margin of the clinopyroxene. Rather, the amphibole mantle is most likely a newly crystallized mineral formed by reaction between surrounding hydrous melts and pre-existing clinopyroxene crystals. This would suggest that the older clinopyroxene core grew in a relatively dry magma, but that the later amphibole mantle grew in a hydrous magma, which is corroborated by the amphibole EMPA data and supports a model of magma mixing. According to the classification of the amphibole (Leake et al., 1997), the amphibole mantles belong to the edenite and magnesiohornblende field (**Figure 11**), namely the magmatic calcic amphibole. Furthermore, the amphibole patches/inclusions within the clinopyroxene core are identified as silicic edenite and actinolite, which could also be employed as evidence of disequilibrium due to the addition of wet melts. Intriguingly, the amphibole patches are linked by numerous needle-like amphiboles, which show a single preferred orientation (**Figures 10B, E, G**). This suggests that the amphibole patches and needles formed by pseudo-exsolution of the pre-existing clinopyroxene, triggered by rapid decompression or cooling. This disequilibrium feature was most likely induced by magma hybridization (Zhang et al., 2013).

The intermediate enclaves comprise rocks of quartz-diorite, tonalite to granodiorite in composition. Generally, these MMEs have a microporphyritic texture defined by large plagioclase crystals (**Figures 7C, D**, **12A–C**; **Supplementary Figure S1E**), large K-feldspar crystals (**Figures 7A,B**), large amphibole crystals (**Figures 12D–F**), bladed biotite crystals (**Figure 12G**), acicular apatite grains (**Figure 12H**) and plagioclase ocelli (**Figure 12I**), as well as clots or clusters of amphibole-biotite crystals (Ma et al., 2017a), set in a finer-grained groundmass that is mainly composed of plagioclase, amphibole, bladed biotite and minor quartz (**Figure 12G**). Bladed biotite, such as observed in the intermediate-composition MMEs, is often used as an indicator of rapid growth and/or physical restriction in a supercooling environment associated with magma mixing conditions (Hibbard, 1991; Kim et al., 2002). In addition, apatite occurs as stubby crystals in the host granitoid rocks, whereas in MMEs it occurs as needles enclosed in other large minerals such as plagioclase phenocrysts (**Figure 12H**). In contrast to the stubby apatite in host granitoids, the acicular apatite of MMEs formed by rapid growth during quenching of a magma (Hibbard, 1991; Barnes et al., 2021). Acicular apatite grains in MMEs therefore provide additional evidence for magma mixing.

The ocellar textures in plagioclase and quartz in MMEs, where ovoid plagioclase or quartz is mantled by finer aggregates of amphibole or bladed biotite crystals (**Figure 12I**), provides further support for magma mixing (Sylvester, 1998; Jiang et al., 2018). The plagioclase ocelli of MMEs are common in the Quxu batholith (Ma et al., 2017a), whereas quartz ocellar texture is scarce. More work focusing on the quartz ocelli is needed in the future.

Disequilibrium textures are also ubiquitous in the host plutons. For instance, the gabbro or norite contains both andesine and labradorite (**Figure 13**; Dong et al., 2006; Wang et al., 2019b; Shui et al., 2021), indicating magma mixing occurred in the Early Eocene Quxu intrusive complex (Wang et al., 2019b).

Based on the above discussion, we support previous studies that have proposed a magma mixing/hybrid origin for the widespread MMEs of the Quxu batholith, and further suggest that some MMEs record additional magma mixing after their formation. In addition, it is important to note that there is no prominent difference in isotopic compositions between the granitoid rocks and the MMEs, suggesting a similar hybrid origin for both the MMEs and the host granitoids: geochemically, most of the MMEs are intermediate in

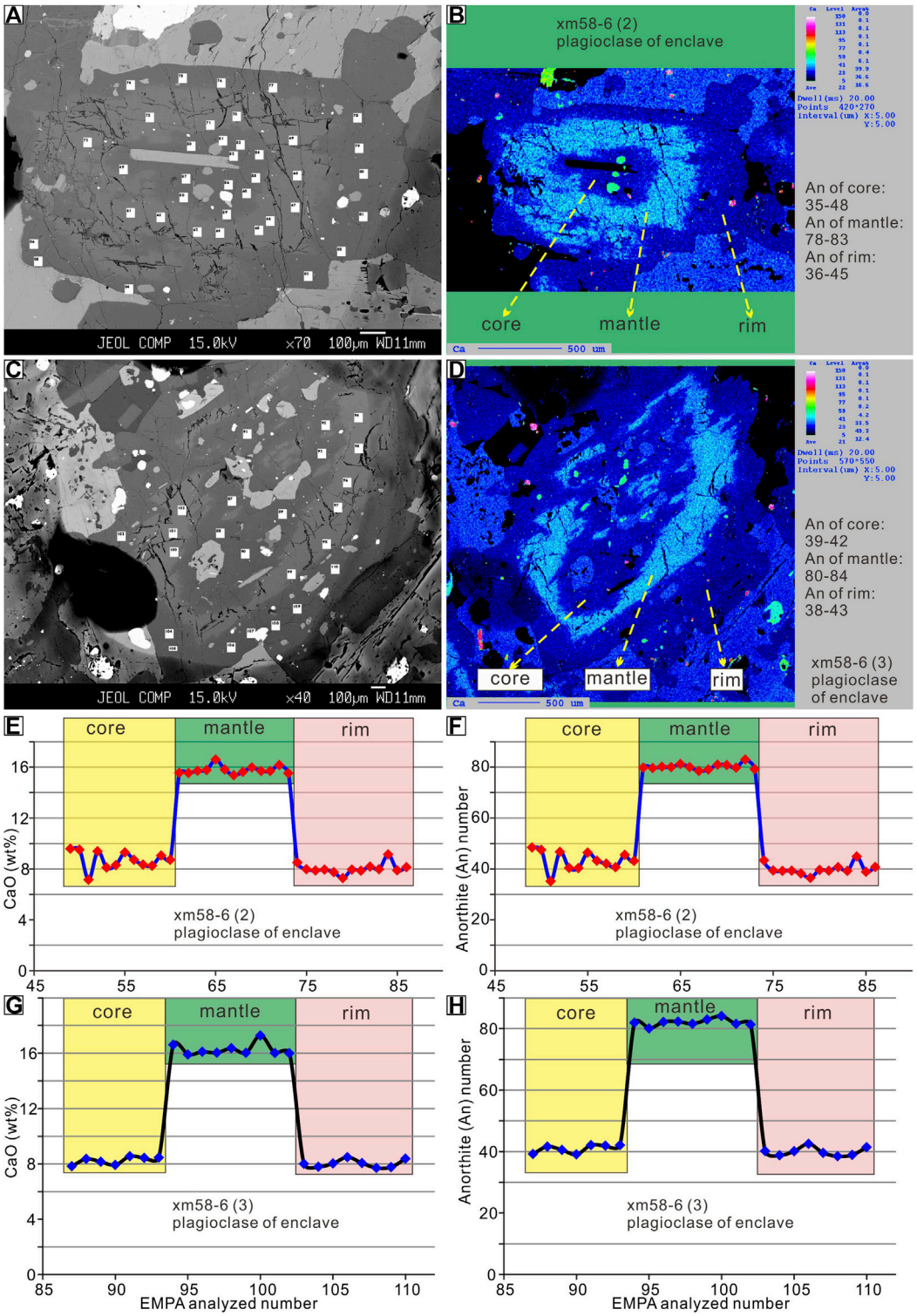

FIGURE 9 | Photomicrographs of plagioclase phenocrysts enclosed within the enclaves. **(A, C)** Backscattered-electron images (BSEs) for these plagioclases, revealing discontinuous zoning. **(B, D)** Electron microprobe analyses (EMPA) compositional mapping for these plagioclase phenocrysts. **(E–H)** CaO contents and anorthite (An) number plotting.

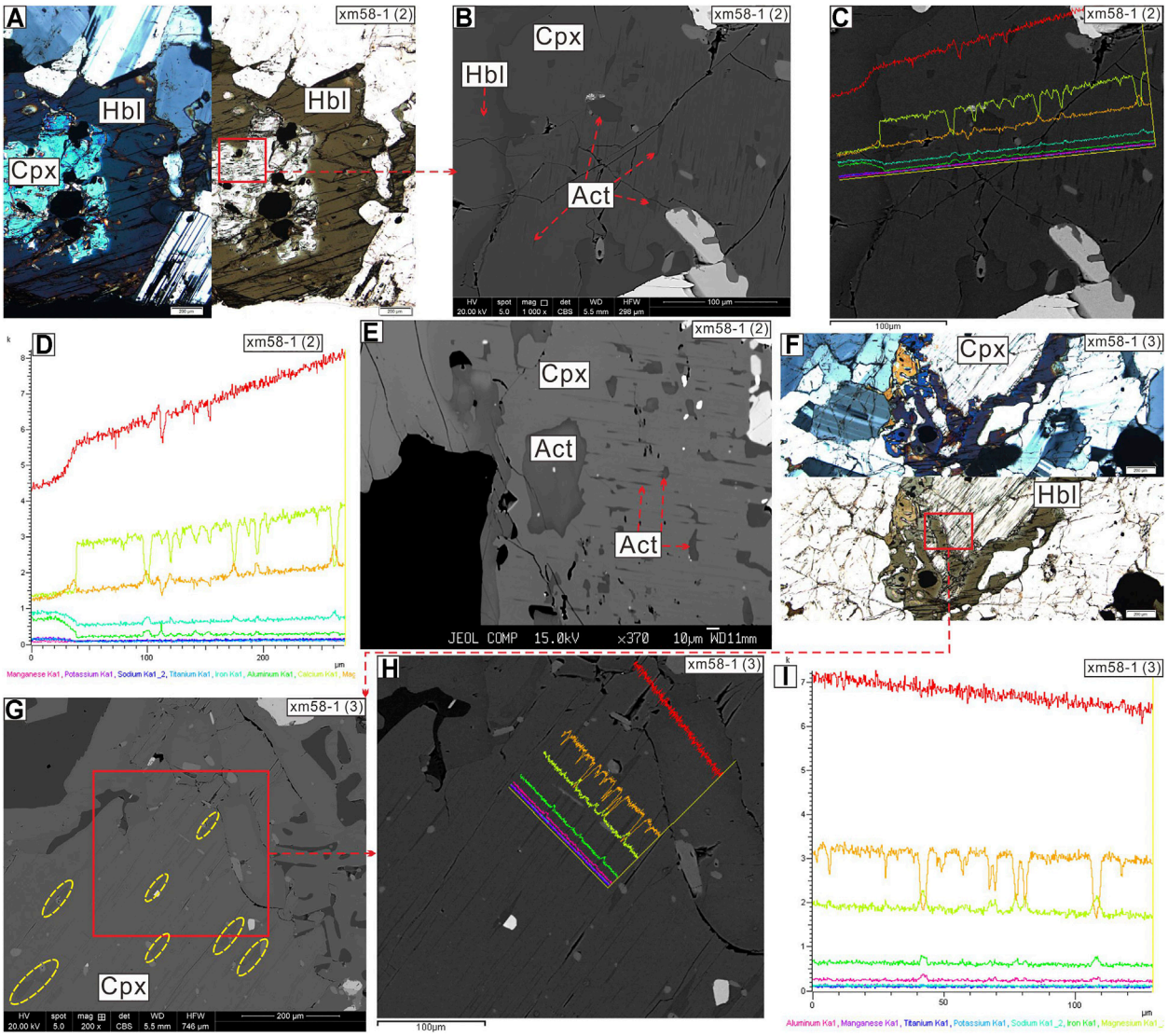

FIGURE 10 | Photomicrographs of the clinopyroxene-amphibole (Cpx-Amp) textures and compositional scans. **(A, F)** Photomicrograph of Cpx-Amp under cross-polarized light and plane-polarized light. **(B, E, G)** BSE image of the close-up area from the Cpx. **(C, D, H, I)** Compositional scan of the Cpx along a line. Abbreviations: Act-actinolite; Amp-amphibole; Cpx-clinopyroxene.

composition, falling into the transitional zone between mafic and felsic end-members in the Harker diagrams (Ma et al., 2017a; Wang et al., 2019b; Wen et al., 2021). Isotopically, most of the granitoid rocks in the Gangdese belt were generated from the fractional crystallization of the juvenile crust, especially the Eocene pluton in the Quxu batholith (Ji et al., 2009; Tang et al., 2021).

Multiple Stages of Magma Hybridization

Based on the field observations, Barbarin (2005) proposed a fourfold model of magma mixing for the central Sierra Nevada batholith: 1) thorough mixing at depth produced homogeneous magmas that crystallized to granitoids, possibly with some MMEs; 2) mingling and local mixing during ascent and emplacement produced the many types of MMEs observed; 3) mingling and limited mixing at the emplacement level produced the MMEs of the composite and strongly hybridized dikes. In the meantime, differentiation or local segregation commonly followed mixing and mingling; and 4) late injections of mafic magma into an essentially solid granitoid rock result in undisturbed mafic dikes. A similar mixing model has been proposed for Neoarchean calc-alkaline magmatic arcs in southern India (Jayananda et al., 2009; Prabhakar et al., 2009; Jayananda et al., 2014).

In the present study, we adapt the above model to illuminate the magma mixing processes in the Quxu batholith, southern Tibet.

The first stage of hybridization: mantle-derived and crust-derived magmas mix thoroughly to generate magma with an intermediate composition. Some workers would doubt the

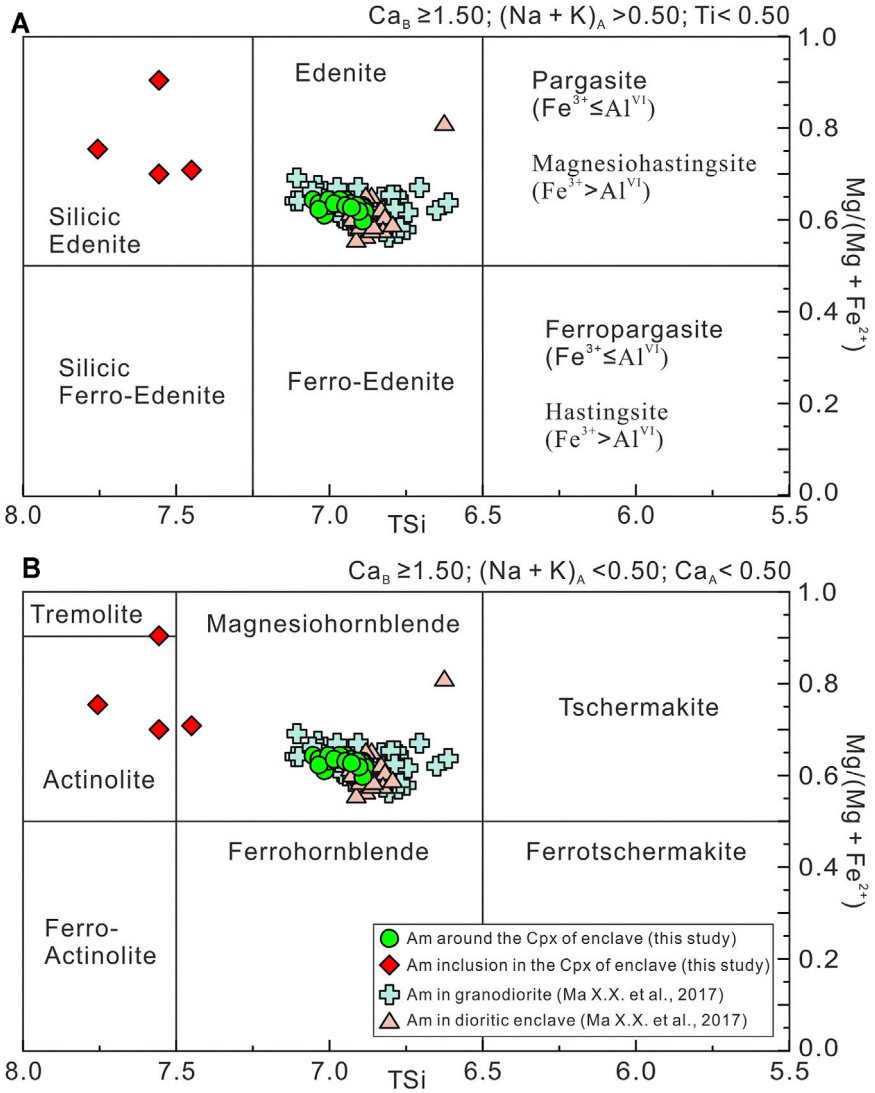

FIGURE 11 | Classification of the amphibole in the present study. **(A,B)** Two diagrams showing the classification of amphiboles according to the nomenclature of Leake et al. (1997).

possibility of mixing between mantle-derived mafic magma and crust-derived felsic magma, because there is a marked contrast between their rheologies, especially the viscosity. However, numerical modeling and experimental work found that when mafic magma is injected into a reservoir from below, the existing magma responds as a viscoplastic material: fault-like surfaces form around the edges of the newly injected magma creating a central mixing zone that can then be fluidized, promoting complex mixing. At a high magma injection rate, the entire mixing zone becomes fluidized. Circulation and/or convection within the mixing zone will bring together minerals from different portions of the reservoir that may have experienced different physiochemical environments, leaving little melt unmixed (Bergantz et al., 2015). In addition, volatile segregation and the rising of bubbles (Wiesmaier et al., 2015), especially from the volatile-rich mantle-derived mafic magma (Capriolo et al., 2020); particle settling (Renggli et al., 2016); magmatic and thermal convection (Weinberg, 2001; Holness et al., 2017; Paterson et al., 2018); and the addition of new pulses or magma batches (Ardill et al., 2020) are other favorable mechanisms encouraging the magma mixing between mafic and felsic magma end-members. Therefore, underplating of mantle-derived basaltic magma, providing pulses of new magma and enough heat to perturb a mixing zone, can provide the conditions to allow mixing between mafic and felsic magmas at depth (Jayananda et al., 2014).

The lines of evidence for thorough mixing at depth in the Quxu batholith include: 1) most of the MMEs are quartz diorite to tonalite in composition, resembling the enclosing quartz diorite and tonalite in the Quxu batholith; 2) most of the MMEs are microporphyritic in texture, with large amphibole crystals with discontinuous zoning (Ma et al., 2020a); 3) some of the MMEs

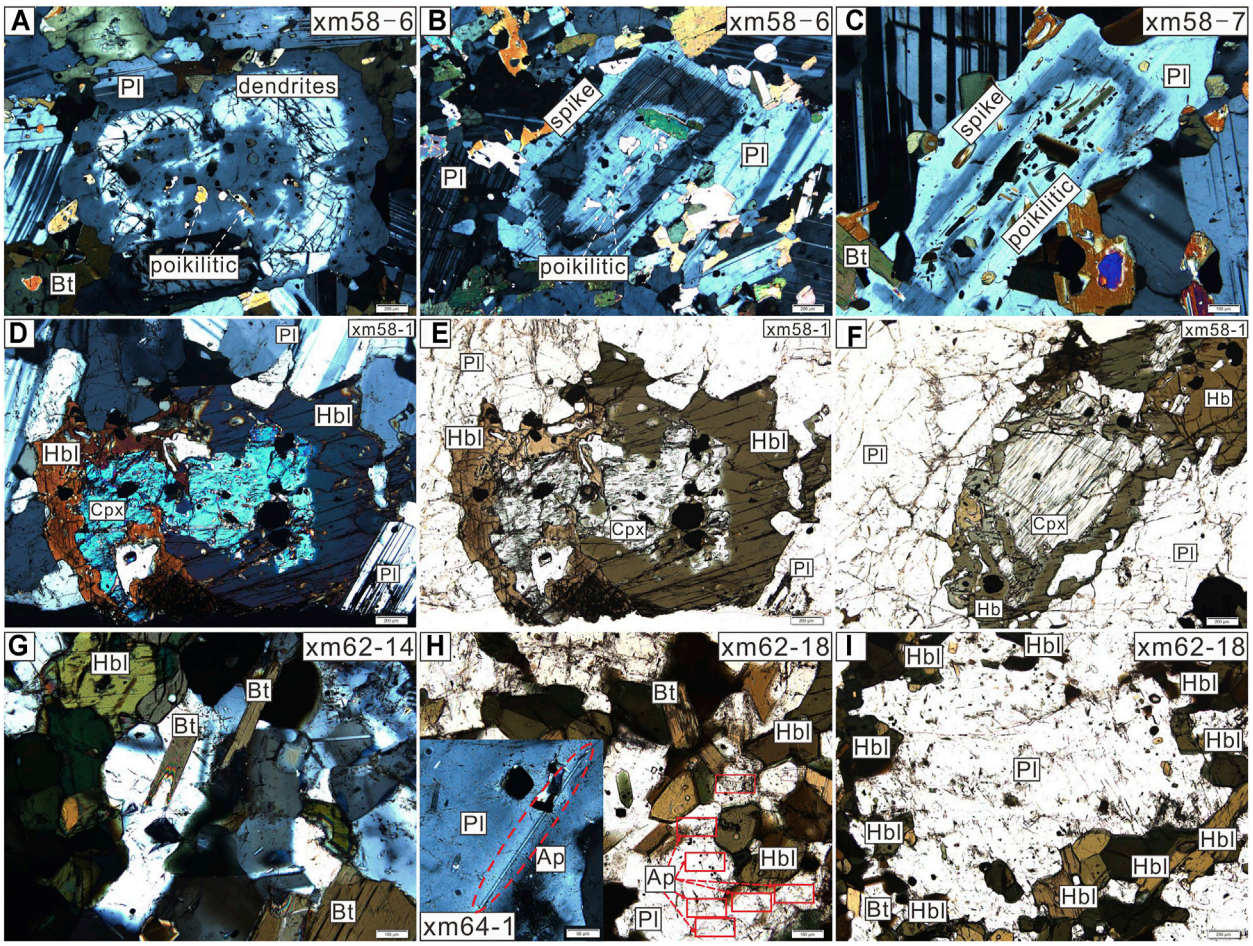

FIGURE 12 | Photomicrographs of plagioclase phenocryst, Cpx-Amp texture, bladed biotite, acicular apatite, and plagioclase ocelli in enclaves. **(A–C)** Photomicrographs of plagioclase phenocrysts showing discontinuous zoning, dendritic and poikilitic textures. **(D–F)** Cpx-Amp core-mantle texture in the enclaves. **(G)** Bladed biotite. **(H)** Acicular apatite enclosed within the plagioclase. **(I)** Plagioclase ocelli, mantled by small hornblende crystals and bladed biotite lathes.

contain large clinopyroxene crystals or clinopyroxene relict cores (with Mg# around 70) (**Figures 12D–F**); 4) occasionally, the host diorite or granodiorite hosts clinopyroxene crystals with Mg# values varying from 65 to 73 (Shu et al., 2018), resembling the clinopyroxene crystals in the MMEs (Shu et al., 2018; Wen et al., 2021) and those in the gabbro, norite and gabbronorite (Wang et al., 2019b; Shui et al., 2021); 5) the MMEs contain plagioclase or plagioclase mantles with anorthite numbers >80 (**Figure 9**; Ma et al., 2017a), similar to those in the mafic rocks (Shu et al., 2018; Wang et al., 2019b; Shui et al., 2021; Wen et al., 2021); and 6) the host granodiorite contains plagioclase with anorthite number >80, whereas the gabbro contains andesine with anorthite numbers of ~45 (**Figure 13**; Dong et al., 2006; Wang et al., 2019b; Wen et al., 2021). All of these observations indicate that most of the MMEs and their enclosing granitoids were sourced from the same homogeneous hybrid magma system, which is a product of magma mixing between mantle-derived and crust-derived melts (Barbarin, 2005; Jayananda et al., 2014; Ma et al., 2020a). Furthermore, the original mafic and felsic components are obscure, and the Hf, Sr, Nd, and O isotopes indicate that most of the Quxu calc-alkaline granitoid magmas were initially hybrids produced by mixing of mantle-derived mafic materials and crustal felsic melts (Dong et al., 2006; Ji et al., 2009; Wang et al., 2019b).

The second stage of hybridization: widespread mingling and/or local mixing during magma ascent and emplacement. During this stage, various types of MMEs are formed. If the injection rate of mafic or hybrid magma into the felsic host magma is slow, the viscosities of the contrasting magmas can be sufficiently distinct from each other to prevent mixing, resulting only in mingling (Barbarin, 2005). In addition, mafic or hybrid magma that was injected into an open system in which felsic magma was already moving upward may not have enough time to thoroughly mix with the felsic host. Therefore, the mafic and hybrid magmas may simply break up into small magma blobs, which will be scattered in the felsic magma to form magma globules, namely the MMEs. These globules move upwards together with the rising felsic magma, with additional globules continually produced due to ongoing heating and disturbance driven by basaltic underplating (Mo et al., 2007). Thus, we can see numerous MMEs enclosed

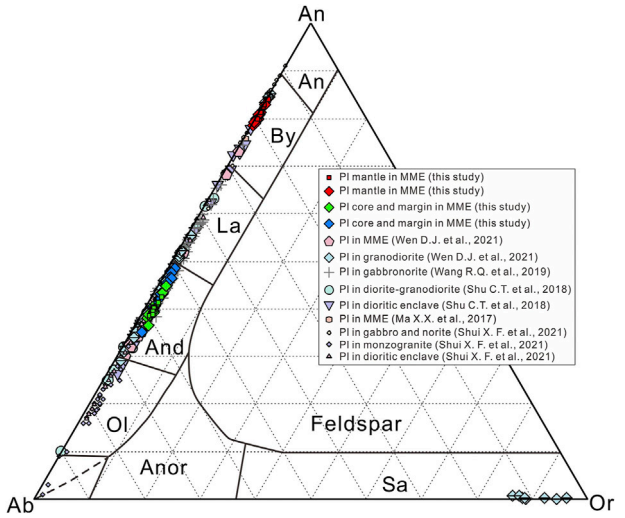

FIGURE 13 | Chemical classification of plagioclase on a ternary diagram (anorthite-albite-orthoclase) for plagioclase. Abbreviations: An, anorthite; And, andesine; Anor, anorthoclase; By, bytownite; La, labradorite; Ol, oligoclase; Sa, sanidine.

within the host granitoids, representing mingling of mafic and hybrid magmas with the host felsic magma. The mingling increases the contact surface area between the MMEs and host granitoid magma and promotes thermal, mineral, and chemical transfer between these two components, resulting in local mixing between each globule of mafic or hybrid magma and the enclosing granitoid magma.

The wide variety of MMEs in the Quxu batholith likely crystallized from multiple batches of hybrid magmas related to distinct mixing events that involved different proportions of the end members. In the Quxu batholith, the large volumes of mafic magma probably delayed crystallization of the granitoid magma system and enabled efficient mixing and mingling over a protracted time, further contributing to MME diversity (Mo et al., 2007; Dong, 2008; Mo et al., 2009). Local mixing during ascent and emplacement may explain the similar chemical and mineralogical traits of each host-MME pair and the differences between the various pairs in the same intrusion. Polygenic swarms that include various types of MMEs should be distinguished from monogenic swarms in which the MMEs are similar and formed at the same time (**Figures 3A–D**). The various types of MMEs may then have aggregated together to form variable swarms (**Figures 4D–F**). Other relatively solid particles (crystals or xenoliths) that were present in the granitoid magma were also prone to be concentrated into the swarms. These polygenic swarms are generally concentrated near the margins of the plutons because, in flowing magma, they more easily form lag deposits between domains of contrasting components with different temperatures and rheologies (Barbarin, 2005).

The final stage of hybridization: local mingling and limited mixing at the emplacement level. At this level, early fractures within incompletely crystallized granitoids will channel the residual liquid and fluids. Mafic and/or hybrid magmas, injected into the fractures, will initially form synplutonic dikes. With ongoing magmatic flow, however, the mafic or hybrid magma will be fragmented into globules and interact with the residual melts. Enclave swarms move along with their host felsic melt during magmatic flow within the fracture system, becoming slightly elongated. However, these enclaves did not escape from the fracture system. In such a case, each fracture becomes a distinct local mixing system with specific physical properties and proportions of the end members, which then produces a certain type of MME. These processes are responsible for much of the great variety of dikes (e.g., synplutonic, composite and undisturbed dikes) and MMEs observed in the Quxu batholith, which were subject to a variety of different formation and evolution processes.

At this stage, the major factors controlling the efficiency of hybridization/mixing within each fracture are the relative physical conditions of the two contrasting components, the timing of mafic magma injection into the fracture, and the amount of felsic melt available. Hybridization of MMEs scattered in a granitoid matrix results in the transfer of crystals, chemical components, and energy between the MME and the host magma (**Figures 7A–D**). Furthermore, the incorporation or interaction between MME and enclosing host will lead to partial or complete isotopic equilibration (Baker, 1989; Lesher, 1990). The occurrence of fine-grained and lobate margins in the mafic blobs reflects the contrasts in physical properties such as viscosity, rheology, and temperature (**Figure 3H**; **Supplementary Figure S2A**). The fine-grained chilled leucocratic margins of the MMEs limited further mineral and chemical exchange (**Figure 7D**). Due to this isolation of the leucocratic margin, complete isotopic equilibration is prohibited between enclaves and their enclosing host granitoids once a chilled margin is formed.

Geodynamic Significance

The Quxu batholith was emplaced largely between 55 and 45 Ma (peaking at ca. 50 Ma), corresponding to the Early Eocene magma flare-up event in the Gangdese belt, southern Tibet (Wen et al., 2008; Zhu et al., 2019; Ma et al., 2021a; Ma et al., 2021b). This magma flare-up event occurred during the main stage of Indo-Asian collision (Hu et al., 2015). The magma mixing process mainly took place at ca. 50 Ma, confirmed by the coeval crystallizing ages for both the host granitoids and enclosed MMEs (Mo et al., 2005; Ma et al., 2017a; Shu et al., 2018; Wang et al., 2019b; Shui et al., 2021; Wen et al., 2021). However, the question remains: what kind of geodynamic regime could be employed to explain this magma mixing?

Regarding the felsic crustal material, numerous previous studies have found that the Early Eocene (55–45 Ma) granitoid rocks of the Gangdese belt show clear arc-affinity characteristics: calc-alkaline geochemistry, depleted whole-rock Sr-Nd, and O isotopes, as well as depleted zircon Lu-Hf isotopes (Meng et al., 2018a; Zhou et al., 2018; Guo et al., 2019; Ma et al., 2021a; Ma et al., 2021b; Tang et al., 2021). These geochemical indicators reveal that these igneous rocks were generated from partial melting of mantle wedge and juvenile crust in a subduction-

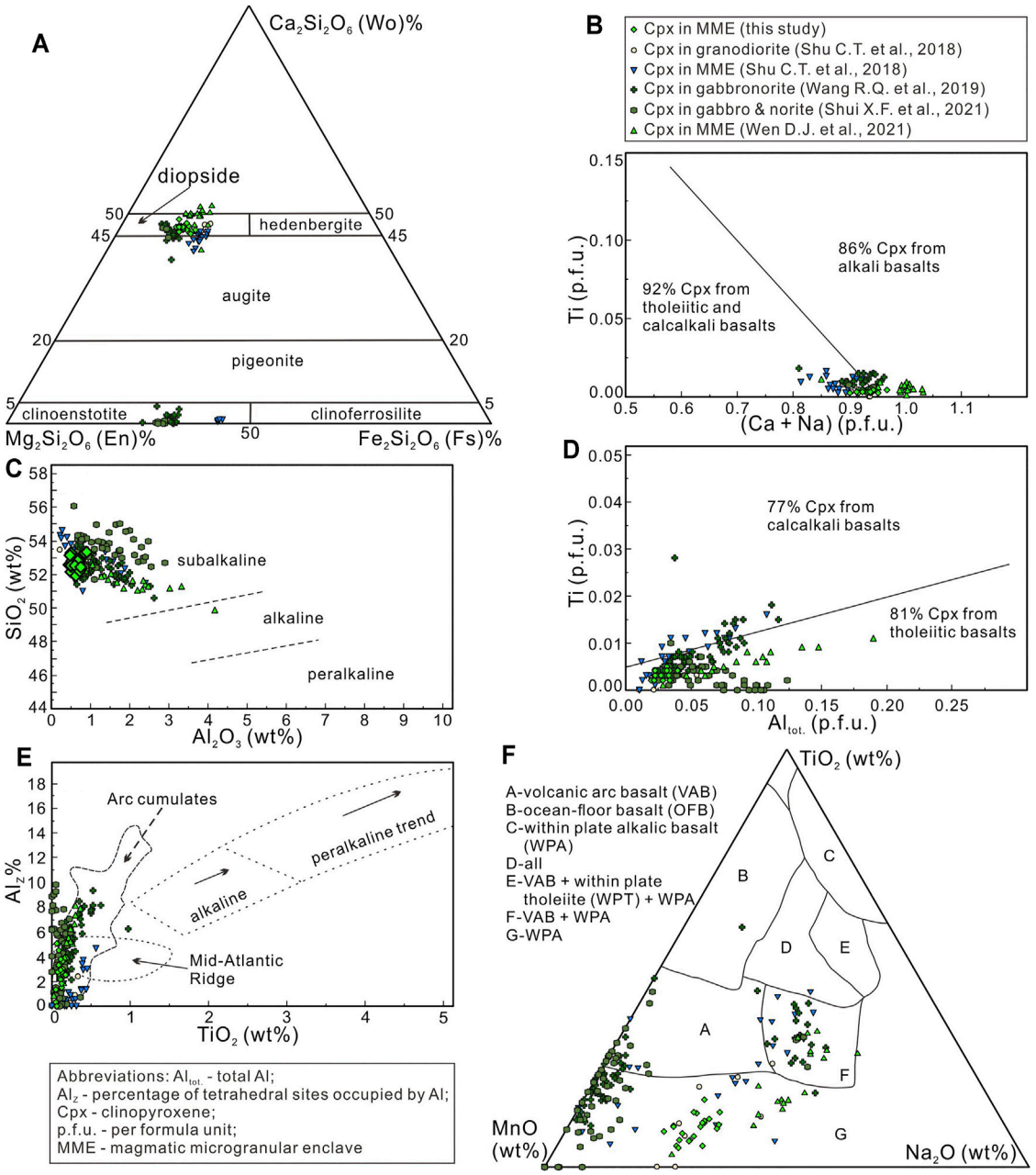

FIGURE 14 | Classification and tectonic discrimination of clinopyroxene. **(A)** Classification of clinopyroxene according to the nomenclature of Morimoto (1988). **(B)** Discrimination diagram for clinopyroxene phenocrysts from alkaline basalts and other basalts (Leterrier et al., 1982). **(C)** SiO_2-Al_2O_3 covariation in clinopyroxenes from different magma types (Nisbet and Pearce, 1977). **(D)** Discrimination diagram of clinopyroxenes from calc-alkali basalts and tholeiitic basalts (Leterrier et al., 1982). **(E)** Al_Z (percentage of tetrahedral sites occupied by Al) vs. wt% TiO_2 in clinopyroxene (Loucks, 1990). **(F)** Triangular diagram of TiO_2-MnO-Na_2O for discriminating between pyroxenes from different magma types (Nisbet and Pearce, 1977).

related arc setting. The juvenile crust may have included Late Cretaceous juvenile mafic arc crust (Tang et al., 2021) and the Middle Triassic gabbro-dioritic plutons (Ma et al., 2020b). Intriguingly, the 48–49 Ma Quxu batholith yielded similar weighted mean ages of depleted mantle modal ages (T_{DM1}) of ~290 Ma to the ~300 Ma weighted mean age of T_{DM1} for the ~240 Ma Renbu gabbro-dioritic pluton (Ma et al., 2017a; Ma et al., 2020b). In contrast with the Early Eocene granitoids, the Late Eocene (<43 Ma) granitoids exhibit more evolved whole-rock Sr-Nd-Hf isotope compositions, indicating derivation from a mixed source of juvenile arc crust and ancient continental crust (Shui et al., 2021; Tang et al., 2021). At ca. 43 Ma, strongly fractionated granite was emplaced in the western Gangdese belt. This granite is thought to be derived from partial melting of

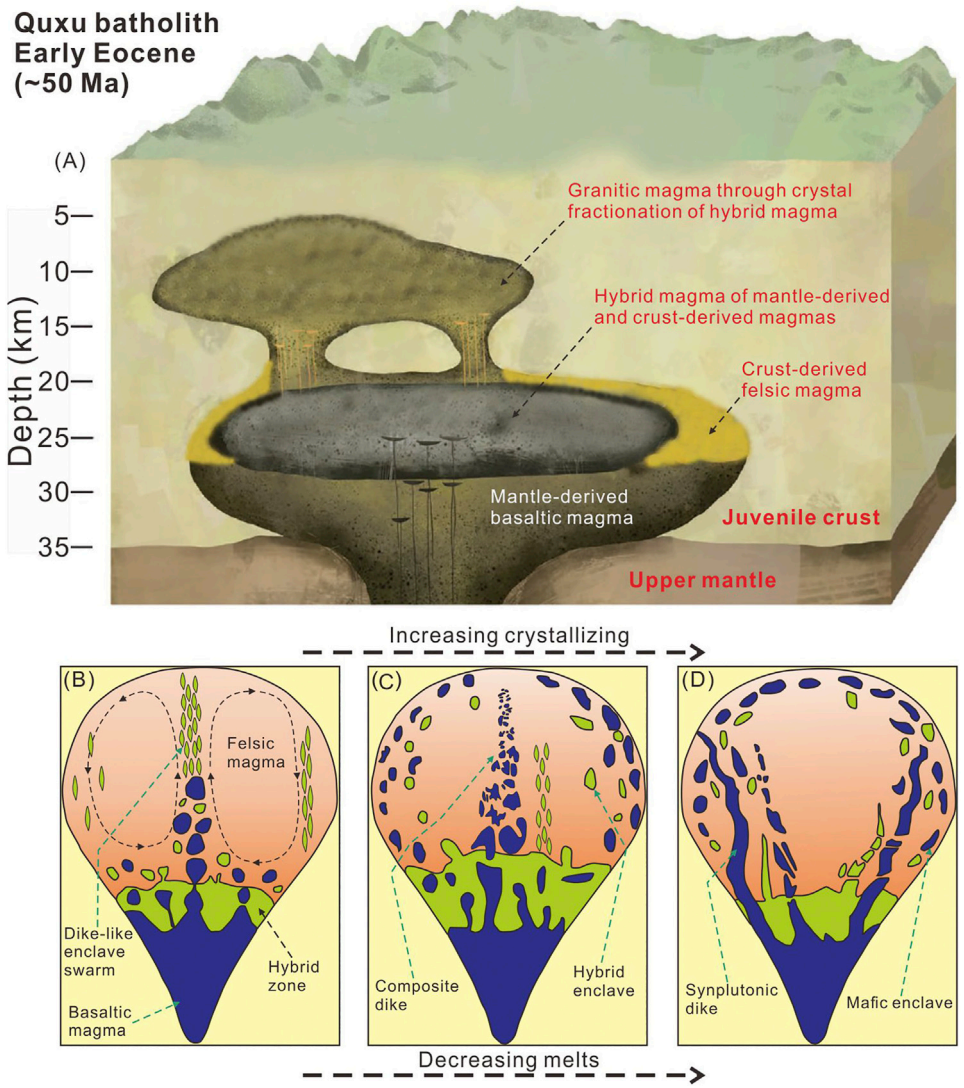

FIGURE 15 | Proposed model for the formation processes of multiple stages of magma mixing/hybridizations. **(A)** Overview of the magma mixing at depth (modified from Bachmann and Huber (2016)). **(B–D)** Detailed illustration of the processes of magma hybridization and the various types of resulting enclaves and dikes (modified from Barbarin (2005), Jayananda et al. (2014)).

garnet-bearing amphibolite within the juvenile southern Lhasa crust and mixed with enriched components from the subducting ancient Indian continental crust (Wang et al., 2015). The involvement of the ancient Indian continental crust was further corroborated by the abundance of inherited zircons within the ca. 41 Ma dioritic dikes and the ca. 40 Ma granite in the Gangdese belt (Ma et al., 2016; Laskowski et al., 2017).

In short, the felsic crust-derived melts, as an end-member of the Early Eocene magma mixing of the Quxu batholith, originate from the partial melting of the juvenile crust (**Figure 15A**). The partial melting event occurred during the waning stage of subduction of the Neotethyan oceanic slab beneath the Lhasa terrane (Guo et al., 2012; Wang et al., 2019b; Tang et al., 2021).

The mafic mantle-derived magma, as the second end-member of the Early Eocene magma mixing in the Quxu batholith (**Figure 15A**), is represented by the coeval MMEs and the scattered gabbro, norite, and gabbronorite plutons in the Quxu batholith. Geochemically, the mafic rocks are FeO^T enriched and belong to the low-K tholeiites series with strong similarities to those rocks formed through partial melting of MORB (Wang et al., 2019b). Isotopically, these mafic rocks fall into the field of the Neotethyan ophiolite (Xu and Castillo, 2004; Zhang et al., 2005).

The scattered clinopyroxene crystals in the MMEs, gabbroic series rocks, and granodiorite represent pre-mixing minerals crystallized from the mafic end-member magma. Thus, they are effective tracers of the regional tectonic settings (Leterrier et al., 1982; Loucks, 1990; Nisbet and Pearce, 1977). The new and

compiled compositions of the clinopyroxenes show that they comprise diopside, augite, and clinoenstotite (**Figure 14A**; Morimoto, 1988), resembling the tholeiitic to subalkaline trend (**Figures 14B–D**). In the discriminate diagrams, these clinopyroxenes plot in the overlap area of arc-related and rift-related series (**Figure 14E**; Loucks, 1990), in good agreement with the transition from subduction to intraplate environments (**Figure 14F**; Nisbet and Pearce, 1977). Given the above-mentioned results, these mafic rocks were probably derived from the decompression melting of the upwelling asthenosphere (**Figure 15A**; Dong, 2008; Wang et al., 2019b), which may have been triggered by the slab breakoff due to the Indo-Asian collision (Zhu et al., 2015; Ji et al., 2016).

Considering the petrographic, mineralogical, and geochemical data, as well as the regional geology, a tentative model can be proposed for the origin and evolution of the Quxu granitoids and the associated mafic rocks including MMEs (**Figure 15**). This model denotes three stages: 1) mantle-derived mafic magma thoroughly mixes with a crustal felsic component to create hybrid magma, which then fractionates to produce the different granitoids of the Quxu batholith (**Figures 15A,B**; Ma et al., 2020a); 2) mingling occurs and leads to the formation of MMEs when contrasting physical conditions inhibit thorough mixing between the mafic and felsic components (**Figure 15C**). Local mixing between each MME and host magma results in the enrichment of the MME in K-feldspar and quartz; 3) late surges of mafic magma mix with evolved granitoid magmas to produce the hybrid magmas of the dike-like monogenic enclave swarms and composite dikes (**Figure 15D**).

CONCLUDING REMARKS

The Early Eocene Quxu batholith in the Gangdese belt was formed in the transitional regime from subduction of the Neotethyan oceanic slab beneath the Lhasa terrane to Indo-Asian continent-continent collision. Magma mixing between mantle-derived mafic end-member and crustal felsic material played a pivotal role in the formation of the calc-alkaline plutons and their enclosed MMEs of the Quxu batholith. The multiple hybridization processes occurred during three stages: 1) thorough mixing of mantle-derived and crust-derived magmas at depth; 2) mingling and local mixing during hybrid magma ascent and emplacement, producing MMEs with a range of compositions; and 3) mingling and/or limited mixing within synplutonic fractures at the emplacement level to produce composite dikes, strongly hybridized dikes, and undisturbed dikes.

DATA AVAILABILITY STATEMENT

The original contributions presented in the study are included in the article/**Supplementary Material**, further inquiries can be directed to the corresponding author.

AUTHOR CONTRIBUTIONS

XM designed this research. XM compiled data and wrote the first draft of the manuscript. XM, ZZ, WC, HH, and FX analyzed the data. ZZ, WC, HH, FX, TC, and HL made revisions, polished the language, and provided reviews on the first and revised manuscript. All authors have contributed to the paper and approved all the submitted versions.

FUNDING

This study was co-supported by the National Key Research and Development Project "Key scientific issues of transformative technology" (2019YFA0708604), the second Tibetan Plateau Scientific Expedition and Research Program (STEP) Grant (No. 2019QZKK0802), the Key Special Project for Introduced Talents Team of the Southern Marine Science and Engineering Guangdong Laboratory (Guangzhou) (GML2019ZD0201), the National Natural Science Foundation of China (No. 41502198), Research Grants of Chinese Academy of Geological Sciences (J2024), and the Geological Survey of China (DD20190057, DD20190059, DD20190060).

ACKNOWLEDGMENTS

Three reviewers have provided constructive comments that improved the manuscript greatly. Many thanks to Editor Yibo Yang for his efficient handling on this manuscript. Fruitful discussions with Scott Paterson, Zhenyu He, Zuolin Tian, Yibing Li shed enlightening light on some scientific explanations. We thank Bin Shi for zircon CL images and mineral BSE images, Bing Wu for U-Pb dating, Xiaohong Mao for mineral scanning and EMPA analysis. Xiaobao Hu and Zehou Xiao provided great help during the field trip.

SUPPLEMENTARY MATERIAL

The Supplementary Material for this article can be found online at: https://www.frontiersin.org/articles/10.3389/feart.2021.772374/full#supplementary-material

REFERENCES

Alasino, P. H., Ardill, K., Stanback, J., Paterson, S. R., Galindo, C., and Leopold, M. (2019). Magmatically Folded and Faulted Schlieren Zones Formed by Magma Avalanching in the Sonora Pass Intrusive Suite, Sierra Nevada, California. *Geosphere* 15, 1677–1702. doi:10.1130/ges02070.1

Allégre, C. J., Courtillot, V., Tapponnier, P., Hirn, A., Mattauer, M., Coulon, C., et al. (1984). Structure and Evolution of the Himalaya-Tibet Orogenic belt. *Nature* 307, 17–22. doi:10.1038/307017a0

Andersen, T. (2002). Correction of Common lead in U-Pb Analyses that do Not Report 204Pb. *Chem. Geol.* 192, 59–79. doi:10.1016/s0009-2541(02)00195-x

Ardill, K. E., Paterson, S. R., Stanback, J., Alasino, P. H., King, J. J., and Crosbie, S. E. (2020). Schlieren-Bound Magmatic Structures Record Crystal Flow-Sorting in Dynamic Upper-Crustal Magma-Mush Chambers. *Front. Earth Sci.* 8, 190. doi:10.3389/feart.2020.00190

Bachmann, O., and Huber, C. (2016). Silicic Magma Reservoirs in the Earth's Crust. *Am. Mineral.* 101, 2377–2404. doi:10.2138/am-2016-5675

Baker, D. R. (1989). Tracer versus Trace Element Diffusion: Diffusional Decoupling of Sr Concentration from Sr Isotope Composition. *Geochim. Cosmochim. Acta* 53, 3015–3023. doi:10.1016/0016-7037(89)90177-4

Barbarin, B., and Didier, J. (1992). Genesis and Evolution of Mafic Microgranular Enclaves through Various Types of Interaction between Coexisting Felsic and Mafic Magmas. *Earth Environ. Sci. Trans. R. Soc. Edinb.* 83, 145–153. doi:10.1017/s0263593300007835

Barbarin, B. (2005). Mafic Magmatic Enclaves and Mafic Rocks Associated with Some Granitoids of the central Sierra Nevada Batholith, California: Nature, Origin, and Relations with the Hosts. *Lithos* 80, 155–177. doi:10.1016/j.lithos.2004.05.010

Barnes, C. G., Werts, K., Memeti, V., Paterson, S. R., and Bremer, R. (2021). A Tale of Five Enclaves: Mineral Perspectives on Origins of Mafic Enclaves in the Tuolumne Intrusive Complex. *Geosphere* 17, 352–374. doi:10.1130/GES02233.1

Bergantz, G. W., Schleicher, J. M., and Burgisser, A. (2015). Open-System Dynamics and Mixing in Magma Mushes. *Nat. Geosci.* 8, 793–796. doi:10.1038/ngeo2534

Browne, B. L., Eichelberger, J. C., Patino, L. C., Vogel, T. A., Uto, K., and Hoshizumi, H. (2006). Magma Mingling as Indicated by Texture and Sr/Ba Ratios of Plagioclase Phenocrysts from Unzen Volcano, SW Japan. *J. Volcanol. Geotherm. Res.* 154, 103–116. doi:10.1016/j.jvolgeores.2005.09.022

Cao, W., Yang, J., Zuza, A. V., Ji, W.-Q., Ma, X.-X., Chu, X., et al. (2020). Crustal Tilting and Differential Exhumation of Gangdese Batholith in Southern Tibet Revealed by Bedrock Pressures. *Earth Planet. Sci. Lett.* 543, 116347. doi:10.1016/j.epsl.2020.116347

Capriolo, M., Marzoli, A., Aradi, L. E., Callegaro, S., Dal Corso, J., Newton, R. J., et al. (2020). Deep CO2 in the End-Triassic Central Atlantic Magmatic Province. *Nat. Commun.* 11, 1670. doi:10.1038/s41467-020-15325-6

Castro, A., Moreno-Ventas, I., and de La Rosa, J. D. (1990). Microgranular Enclaves as Indicators of Hybridization Processes in Granitoid Rocks, Hercynian Belt, Spain. *Geol. J.* 25, 391–404. doi:10.1002/gj.3350250321

Chung, S.-L., Chu, M.-F., Zhang, Y., Xie, Y., Lo, C.-H., Lee, T.-Y., et al. (2005). Tibetan Tectonic Evolution Inferred from Spatial and Temporal Variations in Post-Collisional Magmatism. *Earth Sci. Rev.* 68, 173–196. doi:10.1016/j.earscirev.2004.05.001

Dodge, F. C. W., and Kistler, R. W. (1990). Some Additional Observations on Inclusions in the Granitic Rocks of the Sierra Nevada. *J. Geophys. Res.* 95, 17841–17848. doi:10.1029/jb095ib11p17841

Dong, G. C. (2008). Gabbros from Southern Gangdese: Implication for Mass Exchange between Mantle and Crust. *Acta Petrologica Sinica* 24, 203–210.

Dong, G. C., Mo, X., Zhao, Z., and Zhu, D-C. (2006). Magma Mixing in Middle Part of Gangdise Magma belt: Evidences from Granitoid Complex. *Acta Petrologica Sinica* 24, 835–844.

Douglas, J. A. V. (1964). Geologic Investigations in East Greenland, Part VII. The Basistoppen Sheet: A Differentiated Basic Sill Enclosed in the Skaergaard Intrusion, East Greenland. *Meddelelser om Grønland* 164, 1–66.

Farner, M. J., Lee, C.-T. A., and Mikus, M. L. (2017). Geochemical Signals of Mafic-Felsic Mixing: Case Study of Enclave Swarms in the Bernasconi Hills Pluton, California. *GSA Bull.* 130, 649–660. doi:10.1130/b31760.1

Foster, D. A., and Hyndman, D. W. (1990). "Chapter 20: Magma Mixing and Mingling between Synplutonic Mafic Dikes and Granite in the Idaho-Bitterroot Batholith," in *The Nature and Origin of Cordilleran Magmatism: Boulder city, Colorado*. Editor J. L. Anderson (Geological Society of America Memoir), 347–358. doi:10.1130/mem174-p347

Gao, P., Zhao, Z.-F., and Zheng, Y.-F. (2016). Magma Mixing in Granite Petrogenesis: Insights from Biotite Inclusions in Quartz and Feldspar of Mesozoic Granites from South China. *J. Asian Earth Sci.* 123, 142–161. doi:10.1016/j.jseaes.2016.04.003

Ghani, A. A. (1998). Occurrence of Synplutonic Dykes from Perhentian Kecil Island, Besut, Terengganu. *Warta Geol.* 24, 65–68.

Guo, L., Zhang, H-F., Harris, N., and Luo, B. (2019). Tectonic Erosion and Crustal Relamination during the India-Asian continental Collision: Insights from Eocene Magmatism in the southeastern Gangdese belt. *Lithos* 346–347, 151–161. doi:10.1016/j.lithos.2019.105161

Guo, L., Zhang, H.-F., Harris, N., Parrish, R., Xu, W.-C., and Shi, Z.-L. (2012). Paleogene Crustal Anatexis and Metamorphism in Lhasa Terrane, Eastern Himalayan Syntaxis: Evidence from U-Pb Zircon Ages and Hf Isotopic Compositions of the Nyingchi Complex. *Gondwana Res.* 21, 100–111. doi:10.1016/j.gr.2011.03.002

Harrison, T. M., Copeland, P., Kidd, W. S. F., and Yin, A. (1992). Raising Tibet. *Science* 255, 1663–1670. doi:10.1126/science.255.5052.1663

Hibbard, M. J. (1991). "Textural Anatomy of Twelve Magma-Mixed Granitoid Systems," in *Enclaves and Granite Petrology*. Editors J. Didier and B. Barbarin (Amsterdam: Elsevier), 431–444.

Holness, M. B., Farr, R., and Neufeld, J. A. (2017). Crystal Settling and Convection in the Shiant Isles Main Sill. *Contrib. Mineral. Petrol.* 172. doi:10.1007/s00410-016-1325-x

Hu, X., Garzanti, E., Moore, T., and Raffi, I. (2015). Direct Stratigraphic Dating of India-Asia Collision Onset at the Selandian (Middle Paleocene, 59 ± 1 Ma). *Geology* 43, 859–862. doi:10.1130/g36872.1

Huang, Y., Ren, M., Jowitt, S. M., Li, G., Fu, J., Zhang, Z., et al. (2021). Middle Triassic Arc Magmatism in the Southern Lhasa Terrane: Geochronology, Petrogenesis and Tectonic Setting. *Lithos* 380–381, 105857. doi:10.1016/j.lithos.2020.105857

Jackson, S. E., Pearson, N. J., Griffin, W. L., and Belousova, E. A. (2004). The Application of Laser Ablation-Inductively Coupled Plasma-Mass Spectrometry to *In Situ* U-Pb Zircon Geochronology. *Chem. Geol.* 211, 47–69. doi:10.1016/j.chemgeo.2004.06.017

Janoušek, V., Bowes, D. R., Braithwaite, C. J. R., and Rogers, G. (2000). Microstructural and Mineralogical Evidence for Limited Involvement of Magma Mixing in the Petrogenesis of a Hercynian High-K Calc-Alkaline Intrusion: the Kozarovice Granodiorite, Central Bohemian Pluton, Czech Republic. *Trans. R. Soc. Edinb. Earth Sci.* 91, 15–26. doi:10.1017/S0263593300007264

Jayananda, M., Gireesh, R. V., Sekhamo, K.-u., and Miyazaki, T. (2014). Coeval Felsic and Mafic Magmas in Neoarchean Calc-Alkaline Magmatic Arcs, Dharwar Craton, Southern India: Field and Petrographic Evidence from Mafic to Hybrid Magmatic Enclaves and Synplutonic Mafic Dykes. *J. Geol. Soc. India* 84, 5–28. doi:10.1007/s12594-014-0106-2

Jayananda, M., Miyazaki, T., Gireesh, R. V., Mahesha, N., and Kano, T. (2009). Synplutonic Mafic Dykes from Late Archaean Granitoids in the Eastern Dharwar Craton, Southern India. *J. Geol. Soc. India* 73, 117–130. doi:10.1007/s12594-009-0007-y

Ji, W.-Q., Wu, F.-Y., Chung, S.-L., Li, J.-X., and Liu, C.-Z. (2009). Zircon U-Pb Geochronology and Hf Isotopic Constraints on Petrogenesis of the Gangdese Batholith, Southern Tibet. *Chem. Geol.* 262, 229–245. doi:10.1016/j.chemgeo.2009.01.020

Ji, W.-Q., Wu, F.-Y., Chung, S.-L., Wang, X.-C., Liu, C.-Z., Li, Q.-L., et al. (2016). Eocene Neo-Tethyan Slab Breakoff Constrained by 45 Ma Oceanic Island basalt-type Magmatism in Southern Tibet. *Geology* 44, 283–286. doi:10.1130/g37612.1

Jiang, D.-S., Xu, X.-S., Xia, Y., and Erdmann, S. (2018). Magma Mixing in a Granite and Related Rock Association: Insight from its Mineralogical, Petrochemical, and "Reversed Isotope" Features. *J. Geophys. Res. Solid Earth* 123, 2262–2285. doi:10.1002/2017jb014886

Jin, C. W. (1986). Inclusions in Granitoid from Quxu, Lhasa, Xizang. *Acta Petrologica Sinica* 2 (2), 23–32.

Kapp, P., and DeCelles, P. G. (2019). Mesozoic-Cenozoic Geological Evolution of the Himalayan-Tibetan Orogen and Working Tectonic Hypotheses. *Am. J. Sci.* 319, 159–254. doi:10.2475/03.2019.01

Kim, J. S., Shin, K. C., and Lee, J. D. (2002). Petrographical Study on the Yucheon Granite and its Enclaves. *Geosci. J.* 6, 289–302. doi:10.1007/bf03020614

Laskowski, A. K., Kapp, P., Ding, L., Campbell, C., and Liu, X. (2017). Tectonic Evolution of the Yarlung Suture Zone, Lopu Range Region, Southern Tibet. *Tectonics* 36, 108–136. doi:10.1002/2016tc004334

Leake, B. E., Woolley, A. R., Arps, C. E. S., Birch, W. D., Gilbert, M. C., Grice, J. D., et al. (1997). Nomenclature of Amphiboles: Report of the Subcommittee on Amphiboles of the International Mineralogical Association, Commission on

New Minerals and mineral Names. *Can. Mineral.* 35, 219–246. doi:10.1127/ejm/9/3/0623

Lesher, C. E. (1990). Decoupling of Chemical and Isotopic Exchange During Magma Mixing. *Nature* 344, 235–237. doi:10.1038/344235a0

Leterrier, J., Maury, R. C., Thonon, P., Girard, D., and Marchal, M. (1982). Clinopyroxene Composition as a Method of Identification of the Magmatic Affinities of Paleo-Volcanic Series. *Earth Planet. Sci. Lett.* 59, 139–154. doi:10.1016/0012-821x(82)90122-4

Liu, L., Qiu, J.-S., and Li, Z. (2013). Origin of Mafic Microgranular Enclaves (MMEs) and Their Host Quartz Monzonites from the Muchen Pluton in Zhejiang Province, Southeast China: Implications for Magma Mixing and Crust-Mantle Interaction. *Lithos* 160–161, 145–163. doi:10.1016/j.lithos.2012.12.005

Loucks, R. R. (1990). Discrimination of Ophiolitic from Nonophiolitic Ultramafic-Mafic Allochthons in Orogenic Belts by the Al/Ti Ratio in Clinopyroxene. *Geology* 18, 346–349. doi:10.1130/0091-7613(1990)018<0346:doofnu>2.3.co;2

Ludwig, K. R. (2003). *User's Manual for Isoplot 3.0: A Geochronological, Toolkit for Microsoft Excel Berkeley Geochronology Center*. Berkeley Geochronology Center, Berkeley special publication, 1–71.

Ma, X., Meert, J. G., Xu, Z., and Yi, Z. (2018). Late Triassic Intra-oceanic Arc System within Neotethys: Evidence from Cumulate Appinite in the Gangdese belt, Southern Tibet. *Lithosphere* 10, 545–565. doi:10.1130/l682.1

Ma, X., Meert, J. G., Xu, Z., and Zhao, Z. (2017a). Evidence of Magma Mixing Identified in the Early Eocene Caina Pluton from the Gangdese Batholith, Southern Tibet. *Lithos* 278–281, 126–139. doi:10.1016/j.lithos.2017.01.020

Ma, X. X., Shi, B., Xiong, F. H., and Li, H. B. (2020a). Magma Mixing of the Quxu Batholith in the Gangdese belt, Southern Tibet: Evidence from Microstructure of Hornblende in Microgranular Enclaves. *Acta Petrologica Sinica* 36, 3063–3080. doi:10.18654/1000-0569/2020.10.08

Ma, X., Xu, Z., and Meert, J. G. (2016). Eocene Slab Breakoff of Neotethys as Suggested by Dioritic Dykes in the Gangdese Magmatic belt, Southern Tibet. *Lithos* 248–251, 55–65. doi:10.1016/j.lithos.2016.01.008

Ma, X., Xu, Z., and Meert, J. G. (2017b). Syn-Convergence Extension in the Southern Lhasa Terrane: Evidence from Late Cretaceous Adakitic Granodiorite and Coeval Gabbroic-Dioritic Dykes. *J. Geodyn.* 110, 12–30. doi:10.1016/j.jog.2017.07.004

Ma, X., Xu, Z., Meert, J. G., Tian, Z., and Li, H. (2021b). Early Eocene High-Flux Magmatism and Concurrent High-Temperature Metamorphism in the Gangdese belt, Southern Tibet. *GSA Bull.* 133, 1194–1216. doi:10.1130/b35770.1

Ma, X., Xu, Z., Zhao, Z., and Yi, Z. (2020b). Identification of a New Source for the Triassic Langjiexue Group: Evidence from a Gabbro-Diorite Complex in the Gangdese Magmatic belt and Zircon Microstructures from Sandstones in the Tethyan Himalaya, Southern Tibet. *Geosphere* 16, 407–434. doi:10.1130/ges02154.1

Ma, X. X., Xu, Z. Q., Liu, F., Zhao, Z. B., and Li, H. B. (2021a). Continental Arc Tempos and Crustal Thickening: a Case Study in the Gangdese Arc, Southern Tibet. *Acta Geol. Sin.* 95, 107–123. doi:10.19762/j.cnki.dizhixuebao.2021007

Meng, Y., Dong, H., Cong, Y., Xu, Z., and Cao, H. (2016). The Early-Stage Evolution of the Neo-Tethys Ocean: Evidence from Granitoids in the Middle Gangdese Batholith, Southern Tibet. *J. Geodynamics* 94-95, 34–49. doi:10.1016/j.jog.2016.01.003

Meng, Y. K., Xu, Z. Q., Gao, C. S., Xu, Y., and Li, R. H. (2018a). The Identification of the Eocene Magmatism and Tectonic Significance in the Middle Gangdese Magmatic belt, Southern Tibet. *Acta Petrol. Sin.* 34, 513–546.

Meng, Y., Santosh, M., Mao, G., Lin, P., Liu, J., and Ren, P. (2020). New Constraints on the Tectono-Magmatic Evolution of the central Gangdese belt from Late Cretaceous Magmatic Suite in Southern Tibet. *Gondwana Res.* 80, 123–141. doi:10.1016/j.gr.2019.10.014

Meng, Y., Xu, Z., Xu, Y., and Ma, S. (2018b). Late Triassic Granites from the Quxu Batholith Shedding a New Light on the Evolution of the Gangdese Belt in Southern Tibet. *Acta Geol. Sin.* 92, 462–481. doi:10.1111/1755-6724.13537

Mitchell, A. A., Eales, H. V., and Johan Kruger, F. (1998). Magma Replenishment, and the Significance of Poikilitic Texlures, in the Lower Main Zone of the Western Bushveld Complex, South Africa. *Mineral. Mag.* 62, 435–450. doi:10.1180/002646198547783

Mo, X., Dong, G., Zhao, Z., Zhu, D., Zhou, S., and Niu, Y. (2009). Mantle Input to the Crust in Southern Gangdese, Tibet, during the Cenozoic: Zircon Hf Isotopic Evidence. *J. Earth Sci.* 20, 241–249. doi:10.1007/s12583-009-0023-2

Mo, X., Hou, Z., Niu, Y., Dong, G., Qu, X., Zhao, Z., et al. (2007). Mantle Contributions to Crustal Thickening during continental Collision: Evidence from Cenozoic Igneous Rocks in Southern Tibet. *Lithos* 96, 225–242. doi:10.1016/j.lithos.2006.10.005

Mo, X. X., Dong, G., Zhao, Z., Guo, T., Wang, L., Chen, T., et al. (2005). Timing of Magma Mixing in the Gangdise Magmatic belt during the India-Asia Collision: Zircon SHRIMP U-Pb Dating. *Acta Geol. Sin.* 79, 66–76.

Mo, X. X., Zhao, Z., Deng, J. F., and Dong, G. (2003). Response of Volcanism to the India-Asia Collision. *Earth Sci. Front.* 10, 135–148.

Morimoto, N. (1988). Nomenclature of Pyroxenes. *Mineral. Petrol.* 39, 55–76. doi:10.1007/bf01226262

Nelson, S. T., and Montana, A. (1992). Sieve-Textured Plagioclase in Volcanic Rocks Produced by Rapid Decompression. *Am. Mineral.* 77, 1242–1249.

Nisbet, E. G., and Pearce, J. A. (1977). Clinopyroxene Composition in Mafic Lavas from Different Tectonic Settings. *Contrib. Mineral. Petrol.* 63, 149–160. doi:10.1007/bf00398776

Niu, Y., Zhao, Z., Zhu, D.-C., and Mo, X. (2013). Continental Collision Zones Are Primary Sites for Net continental Crust Growth - A Testable Hypothesis. *Earth Sci. Rev.* 127, 96–110. doi:10.1016/j.earscirev.2013.09.004

Paterson, S. R., Ardill, K., Vernon, R., and Žák, J. (2018). A Review of Mesoscopic Magmatic Structures and Their Potential for Evaluating the Hypersolidus Evolution of Intrusive Complexes. *J. Struct. Geol.* 125, 134–147. doi:10.1016/j.jsg.2018.04.022

Pin, C., Binon, M., Belin, J. M., Barbarin, B., and Clemens, J. D. (1990). Origin of Microgranular Enclaves in Granitoids: Equivocal Sr-Nd Evidence from Hercynian Rocks in the Massif Central (France). *J. Geophys. Res.* 95, 17821–17828. doi:10.1029/jb095ib11p17821

Prabhakar, B. C., Jayananda, M., Shareef, M., and Kano, T. (2009). Synplutonic Mafic Injections into Crystallizing Granite Pluton from Gurgunta Area, Northern Part of Eastern Dharwar Craton: Implications for Magma Chamber Processes. *J. Geol. Soc. India* 74, 171–188. doi:10.1007/s12594-009-0120-y

Reid, J. B., Jr, and Hamilton, M. A. (1987). Origin of Sierra Nevadan Granite: Evidence from Small Scale Composite Dikes. *Contr. Mineral. Petrol.* 96, 441–454. doi:10.1007/bf01166689

Renggli, C. J., Wiesmaier, S., De Campos, C. P., Hess, K. U., and Dingwell, D. B. (2016). Magma Mixing Induced by Particle Settling. *Contrib. Mineral. Petrol.* 171 (96), 96–13. doi:10.1007/s00410-016-1305-1

Shu, C., Long, X., Yin, C., Yuan, C., Wang, Q., He, X., et al. (2018). Continental Crust Growth Induced by Slab Breakoff in Collisional Orogens: Evidence from the Eocene Gangdese Granitoids and Their Mafic Enclaves, South Tibet. *Gondwana Res.* 64, 35–49. doi:10.1016/j.gr.2018.06.004

Shui, X.-F., Klemd, R., He, Z.-Y., Mao, J.-W., and Zhao, Y.-Y. (2021). Geochronology and Petrogenesis of Eocene Gabbros and Granitic Rocks of the Eastern Gangdese belt, Southern Tibet: Implications for the Timing of India-Asia Collision. *Gondwana Res.* 97, 145–157. doi:10.1016/j.gr.2021.05.019

Słaby, E., Götze, J., Wörner, G., Simon, K., Wrzalik, R., and Śmigielski, M. (2008). K-feldspar Phenocrysts in Microgranular Magmatic Enclaves: A Cathodoluminescence and Geochemical Study of crystal Growth as a Marker of Magma Mingling Dynamics. *Lithos* 105, 85–97. doi:10.1016/j.lithos.2008.02.006

Sylvester, A. G. (1998). Magma Mixing, Structure, and Re-evaluation of the Emplacement Mechanism of Vrådal Pluton, central Telemark, Southern Norway. *Norsk Geologisk Tidsskrift* 78, 259–276.

Tang, Y.-W., Chen, L., Zhao, Z.-F., and Zheng, Y.-F. (2021). Origin of Syn-Collisional Granitoids in the Gangdese Orogen: Reworking of the Juvenile Arc Crust and the Ancient continental Crust. *GSA Bull.* [Epub ahead of print]. doi:10.1130/B35928.1

Tobisch, O. T., McNulty, B. A., and Vernon, R. H. (1997). Microgranitoid Enclave Swarms in Granitic Plutons, central Sierra Nevada, California. *Lithos* 40, 321–339. doi:10.1016/s0024-4937(97)00004-2

Ueno, K. (2003). The Permian Fusulinoidean Faunas of the Sibumasu and Baoshan Blocks: Their Implications for the Paleogeographic and Paleoclimatologic Reconstruction of the Cimmerian Continent. *Palaeogeogr. Palaeoclimatol. Palaeoecol.* 193, 1–24. doi:10.1016/s0031-0182(02)00708-3

Veevers, J. J., and Tewari, R. C. (1995). Permian-Carboniferous and Permian-Triassic Magmatism in the Rift Zone Bordering the Tethyan Margin of Southern Pangea. *Geology* 23, 467–470. doi:10.1130/0091-7613(1995)023<0467:pcaptm>2.3.co;2

Vernon, R. H. (1990). Crystallization and Hybridism in Microgranitoid Enclave Magmas: Microstructural Evidence. *J. Geophys. Res.* 95, 17849–17859. doi:10.1029/jb095ib11p17849

Vernon, R. H. (2007). Problems in Identifying Restite in S-type Granites of southeastern Australia, with Speculations on Sources of Magma and Enclaves. *Can. Mineral.* 45, 147–178. doi:10.2113/gscanmin.45.1.147

Wang, C., Ding, L., Zhang, L.-Y., Ding, X.-L., and Yue, Y.-H. (2019a). Early Jurassic High-Mg Andesites in the Quxu Area, Southern Lhasa Terrane: Implications for Magma Evolution Related to a Slab Rollback of the Neo-Tethyan Ocean. *Geol. J.* 54, 2508–2524. doi:10.1002/gj.3309

Wang, C., Ding, L., Zhang, L.-Y., Kapp, P., Pullen, A., and Yue, Y.-H. (2016). Petrogenesis of Middle-Late Triassic Volcanic Rocks from the Gangdese belt, Southern Lhasa Terrane: Implications for Early Subduction of Neo-Tethyan Oceanic Lithosphere. *Lithos* 262, 320–333. doi:10.1016/j.lithos.2016.07.021

Wang, Q., Zhu, D.-C., Cawood, P. A., Zhao, Z.-D., Liu, S.-A., Chung, S.-L., et al. (2015). Eocene Magmatic Processes and Crustal Thickening in Southern Tibet: Insights from Strongly Fractionated Ca. 43Ma Granites in the Western Gangdese Batholith. *Lithos* 239, 128–141. doi:10.1016/j.lithos.2015.10.003

Wang, R.-Q., Qiu, J.-S., Yu, S.-B., Lin, L., and Xu, H. (2019b). Magma Mixing Origin for the Quxu Intrusive Complex in Southern Tibet: Insights into the Early Eocene Magmatism and Geodynamics of the Southern Lhasa Subterrane. *Lithos* 328–329, 14–32. doi:10.1016/j.lithos.2019.01.019

Weinberg, R. F. (2001). Magma Flow within the Tavares Pluton, Northeastern Brazil: Compositional and Thermal Convection. *GSA Bull.* 113, 508–520. doi:10.1130/0016-7606(2001)113<0508:mfwttp>2.0.co;2

Wen, D.-J., Hu, X.-M., Qiu, J.-S., Yu, J.-H., Wang, R.-Q., He, Z.-Y., et al. (2021). Petrogenesis of Early Eocene Granites and Associated Mafic Enclaves in the Gangdese Batholith, Tibet: Implications for Net Crustal Growth in Collision Zones. *Lithos* 394–395, 106170. doi:10.1016/j.lithos.2021.106170

Wen, D., Liu, D., Chung, S., Chu, M., Ji, J., Zhang, Q., et al. (2008). Zircon SHRIMP U-Pb Ages of the Gangdese Batholith and Implications for Neotethyan Subduction in Southern Tibet. *Chem. Geol.* 252, 191–201. doi:10.1016/j.chemgeo.2008.03.003

Wiebe, R. A., Blair, K. D., Hawkins, D. P., and Sabine, C. P. (2002). Mafic Injections, *In Situ* Hybridization, and crystal Accumulation in the Pyramid Peak Granite, California. *GSA Bull.* 114, 909–920. doi:10.1130/0016-7606(2002)114<0909:miisha>2.0.co;2

Wiesmaier, S., Morgavi, D., Renggli, C. J., Perugini, D., De Campos, C. P., Hess, K.-U., et al. (2015). Magma Mixing Enhanced by Bubble Segregation. *Solid Earth* 6, 1007–1023. doi:10.5194/se-6-1007-2015

Xie, F., and Tang, J. (2021). The Late Triassic-Jurassic Magmatic belt and its Implications for the Double Subduction of the Neo-Tethys Ocean in the Southern Lhasa Subterrane, Tibet. *Gondwana Res.* 97, 1–21. doi:10.1016/j.gr.2021.05.007

Xu, J.-F., and Castillo, P. R. (2004). Geochemical and Nd-Pb Isotopic Characteristics of the Tethyan Asthenosphere: Implications for the Origin of the Indian Ocean Mantle Domain. *Tectonophysics* 393, 9–27. doi:10.1016/j.tecto.2004.07.028

Xu, W., Zhu, D.-C., Wang, Q., Weinberg, R. F., Wang, R., Li, S.-M., et al. (2021). Mafic Microgranular Enclaves Formed by Gas-Driven Filter Pressing during Rapid Cooling: An Example from the Gangdese Batholith in Southern Tibet. *J. Petrol.* 61. doi:10.1093/petrology/egab003

Xu, Z., Dilek, Y., Cao, H., Yang, J., Robinson, P., Ma, C., et al. (2015). Paleo-Tethyan Evolution of Tibet as Recorded in the East Cimmerides and West Cathaysides. *J. Asian Earth Sci.* 105, 320–337. doi:10.1016/j.jseaes.2015.01.021

Yang, J. S. (2007). Oceanic Subduction-type Eclogite in the Lhasa Block, Tibet, China: Remains of the Paleo-Tethys Ocean Basin? *Geol. Bull. China* 26, 1277–1287.

Yin, A., and Harrison, T. M. (2000). Geologic Evolution of the Himalayan-Tibetan Orogen. *Annu. Rev. Earth Planet. Sci.* 28, 211–280. doi:10.1146/annurev.earth.28.1.211

Zhang, C., Ma, C., Holtz, F., Koepke, J., Wolff, P. E., and Berndt, J. (2013). Mineralogical and Geochemical Constraints on Contribution of Magma Mixing and Fractional Crystallization to High-Mg Adakite-like Diorites in Eastern Dabie Orogen, East China. *Lithos* 172–173, 118–138. doi:10.1016/j.lithos.2013.04.011

Zhang, S.-H., and Zhao, Y. (2017). Cogenetic Origin of Mafic Microgranular Enclaves in Calc-Alkaline Granitoids: The Permian Plutons in the Northern North China Block. *Geosphere* 13, 482–517. doi:10.1130/ges01407.1

Zhang, S.-Q., Mahoney, J. J., Mo, X.-X., Ghazi, A. M., Milani, L., Crawford, A. J., et al. (2005). Evidence for a Widespread Tethyan Upper Mantle with Indian-Ocean-type Isotopic Characteristics. *J. Petrol.* 46, 829–858. doi:10.1093/petrology/egi002

Zhou, L.-m., Wang, R., Hou, Z.-q., Li, C., Zhao, H., Li, X.-W., et al. (2018). Hot Paleocene-Eocene Gangdese Arc: Growth of Continental Crust in Southern Tibet. *Gondwana Res.* 62, 178–197. doi:10.1016/j.gr.2017.12.011

Zhu, D.-C., Wang, Q., Chung, S.-L., Cawood, P. A., and Zhao, Z.-D. (2019). "Gangdese Magmatism in Southern Tibet and India-Asia Convergence Since 120 Ma," in *Himalayan Tectonics: A Modern Synthesis*. Editor P. J. Searle (London: Geological Society, London, Special Publications), 583–604. doi:10.1144/sp483.14

Zhu, D.-C., Wang, Q., Zhao, Z.-D., Chung, S.-L., Cawood, P. A., Niu, Y., et al. (2015). Magmatic Record of India-Asia Collision. *Sci. Rep.* 5, 14289. doi:10.1038/srep14289

Zhu, D.-C., Zhao, Z.-D., Niu, Y., Dilek, Y., Hou, Z.-Q., and Mo, X.-X. (2013). The Origin and Pre-cenozoic Evolution of the Tibetan Plateau. *Gondwana Res.* 23, 1429–1454. doi:10.1016/j.gr.2012.02.002

Zhu, D.-C., Zhao, Z.-D., Niu, Y., Mo, X.-X., Chung, S.-L., Hou, Z.-Q., et al. (2011). The Lhasa Terrane: Record of a Microcontinent and its Histories of Drift and Growth. *Earth Planet. Sci. Lett.* 301, 241–255. doi:10.1016/j.epsl.2010.11.005

Conflict of Interest: The authors declare that the research was conducted in the absence of any commercial or financial relationships that could be construed as a potential conflict of interest.